

**Armorican provenance for the mélange deposits below the Lizard ophiolite  
(Cornwall, UK) – evidence for Devonian obduction of Cadomian and Lower  
Palaeozoic crust onto the southern margin of Avalonia**

Rob A. Strachan<sup>1\*</sup>, Ulf Linnemann<sup>2</sup>, Teresa Jeffries<sup>3</sup>, Kerstin Drost<sup>4</sup>, Jens Ulrich<sup>2</sup>

<sup>1</sup> School of Earth and Environmental Sciences, University of Portsmouth, Portsmouth, PO1 3QL, UK.

<sup>2</sup> Senckenberg Naturhistorische Sammlungen Dresden, Museum für Mineralogie und Geologie, Königsbrücker Landstraße 159, Dresden, D-01109, Germany.

<sup>3</sup> The Natural History Museum, Cromwell Road, London, SW7 5BD, UK.

<sup>4</sup> Universität Tübingen, Fachbereich Geowissenschaften, Isotopengeochemie, Wilhelmstraße 56, Tübingen, D-72076, Germany.

\*corresponding author

**Abstract**

Devonian sedimentary rocks of the Meneage Formation within the footwall of the Lizard ophiolite complex in SW England are thought to have been derived from erosion of the over-riding Armorican microplate during collision with Avalonia and the closure of the Rheic Ocean. We further test this hypothesis by comparison of their detrital zircon suites with those of autochthonous Armorican strata. Five samples analysed from SW England (Avalonia) and NW France (Armorica) have a bimodal U-Pb zircon age distribution dominated by late Neoproterozoic to middle Cambrian (c. 710-518 Ma) and Palaeoproterozoic (c. 1800-2200 Ma) groupings. Both can be linked with lithologies exposed within the Cadomian belt as well as the West African craton, which is characterized by major tectonothermal events at 2.0 to 2.4 Ga. The detrital zircon signature of Avalonia is distinct from that of Armorica in that there is a much larger proportion of Mesoproterozoic detritus. The common provenance of the samples is therefore consistent with: a) derivation of the Meneage Formation mélange deposits from the Armorican plate during Rheic Ocean closure and obduction of the Lizard Complex, and b) previous correlation of quartzite

blocks within the Meneage Formation with the Ordovician Grès Armorica Formation of NW France.

## **Introduction**

Armorica is one of a number of terranes (collectively termed peri-Gondwanan) that were located along the northern Gondwanan margin during the late Neoproterozoic (Fig 1). Together, these terranes record a protracted (c. 780-600 Ma) history of subduction followed at c. 600-550 Ma by a diachronous transition to a continental San Andreas-type transform fault environment, which terminated orogenic activity. In Armorica, this period of orogenic activity is referred to as the Cadomian Orogeny (Bertrand 1921). Development of a stable platform environment followed in the Early Cambrian (e.g. Murphy & Nance 1989, 1991; Taylor & Strachan 1990; Nance et al. 1991, 2002, 2007; Murphy et al. 2000; Keppie et al. 2003). One of these terranes, Avalonia, rifted from the Gondwanan margin during the early Ordovician (Cocks & Torsvik 2002). The subsequent northward drift of Avalonia was associated with the closure of the Iapetus Ocean and the eventual collision of Avalonia with Baltica and Laurentia during the late Ordovician to Silurian to result in the Caledonian orogeny (Pickering et al. 1988; Soper et al. 1992). As Avalonia moved northwards, its southern trailing margin faced a progressively widening oceanic tract known as the Rheic Ocean (e.g. van Staal et al. 1998; Cocks & Torsvik 2002; Stampfli & Borel 2002). The later northward movement of Gondwana and its marginal terranes resulted in closure of the Rheic Ocean during the Devonian-Carboniferous to result in the Variscan orogeny (e.g. Matte 1986). The Rheic Ocean in NW Europe probably closed by south-directed subduction and the collision of Armorica with the southern margin of Avalonia resulted in a north-vergent fold and thrust belt in SW England and southern Ireland (Fig 1; Holder & Leveridge 1986). The Rheic suture is thought to be represented in southwest England (Avalonia) by the ophiolitic rocks of the Lizard Complex (Fig 1) (Nance et al. 2010 and references therein).

Dating of detrital zircons is a powerful tool that can be used to establish the likely provenance of clastic sedimentary rocks and hence assist in the development of palaeogeographic reconstructions (e.g. Rainbird et al. 2001; Fernández-Suárez et

al. 2002a, b; Cawood et al. 2003, 2004, 2007; Murphy et al. 2004; Samson et al. 2005). This is particularly useful where terranes have been detached from their source regions by transcurrent faulting and/or continental rifting and ocean formation. Along the northern Gondwanan margin, for example, the contrasting tectonothermal histories of the Amazonian and West African cratons provide a test for deducing the original location of terranes along that margin (e.g. Fernández-Suárez et al. 2002a, b; Samson et al. 2005). In this paper we present detrital zircon data from Cambrian and Ordovician clastic sedimentary rocks in Armorica (Normandy, NW France) and compare these data with those for rock units of a similar age in other peri-Gondwanan terranes. We also present detrital zircon data from clastic sedimentary rocks within the footwall of the Lizard Complex in SW England. These rock units are thought to have been derived from erosion of the over-riding Armorican microplate during the closure of the Rheic Ocean (Holder & Leveridge 1986; Dorr et al. 1999), and we further test this hypothesis by comparison of their detrital zircon suites with those characteristic of autochthonous Armorican strata.

## **General geology**

### NW France (Armorica)

NW France and the Channel Islands together form the type area of the late Neoproterozoic Cadomian orogenic belt (e.g. Chantraine et al. 1994; Egal et al. 1996; Strachan et al. 1996; Linnemann et al. 2008). This belt is dominated by calc-alkaline plutons and volcanics and variably deformed and metamorphosed volcano-sedimentary sequences of the Brioverian Supergroup (Fig 2). Small areas of Palaeoproterozoic Icartian basement have yielded U-Pb zircon ages of c. 2.2-1.8 Ga for the igneous protoliths (Calvez & Vidal 1978; Samson & D'Lemos 1998). These basement rocks have been correlated with the c. 2.0 Ga Eburnian belt of NW Africa and may represent a detached fragment of the Gondwanan margin (e.g. Cogné 1990; Rabu et al. 1990). Evolution of the Cadomian belt can be divided into four broad phases: a) early subduction-related magmatism (750 and 670-660 Ma); b) syn-



kinematic calc-alkaline plutonism (615-600 Ma); rifting and accumulation of the Brioverian Supergroup (590-570 Ma); and d) regional deformation and metamorphism and continued magmatism (570-540 Ma) (Linnemann et al. 2008 and references therein).

The Cadomian belt is overlain unconformably by transgressive sequences of Cambrian sandstones, siltstones and limestones. These rocks were deposited in fluvial-deltaic to shallow marine environments in basins that were separated from each other by broad landmasses that represented the residual topography after the final stages of Cadomian thickening (Doré 1994). Local occurrences of felsic volcanics are thought to represent the final stages of subduction-related magmatism (Chantraine et al. 1994). During the Arenig, a major marine transgression flooded most of Armorica and deposited an areally extensive quartz sandstone known as the Grès Armoricain Formation (Robardet et al. 1994). This formation is known informally as the 'Armorican Quartzite' and correlative units were also deposited in areas thought to have been contiguous with Armorica such as Iberia, Bohemia, Corsica, Turkey and parts of NW Africa.

One sample of a greywacke turbidite from the Brioverian Supergroup, Sample ROC 1, was collected in Normandy in NW France (Fig 2). Two samples of the Lower Palaeozoic succession in NW France were also collected in Normandy (Fig 2). Sample AM 1 is a quartzite from Lower Cambrian Le Rozel Formation. Sample AM 2 is a quartz sandstone collected from the Grès Armoricain Formation.

#### SW England (Avalonia)

The geology of SW England (Fig 3) is dominated by Devonian and Carboniferous sedimentary successions with minor volcanic units. These rocks were deformed and metamorphosed at low to medium grades during development of the Variscan fold and thrust belt (e.g. Shackleton et al. 1982; Coward & McClay 1983; Leveridge et al. 1984; Sanderson 1984; Seago & Chapman 1988). Deformation commenced at the end of the Devonian or during the early Carboniferous and migrated northwards. As the wave of deformation spread northwards, the thickening orogenic wedge loaded the lithosphere and flexed down the foreland. The Devonian rift basin successions



that were deposited on the southern passive margin of Avalonia were succeeded by Carboniferous clastic sediments that accumulated in foreland basins which were also progressively deformed (Hartley 1993). The post-tectonic S-type granites of the Cornubian Batholith were emplaced during the late Carboniferous to early Permian (Chen et al. 1993; Chesley et al. 1993).

The structurally highest levels of the Variscan belt in SW England are represented by undated orthogneisses of the Eddystone reefs which are assumed to be part of the over-riding Armorican plate (Holder & Leveridge 1986). The underlying Lizard Complex has long been recognized as a tectonically dismembered ophiolite (e.g. Bromley 1979; Styles & Kirby 1980; Vearncombe 1980; Barnes & Andrews 1984, 1986; Floyd 1984; Gibbons & Thompson 1991; Roberts et al. 1993). Its age is best constrained by a U-Pb zircon age of  $397 \pm 2$  Ma obtained from a plagiogranite (Clark et al. 1998). A southerly-inclined crustal-scale structure is interpreted as a Variscan (Rheic) suture which at surface corresponds to the Lizard Complex thrust system (BIRPS & ECORS 1986; Le Gall 1990).

The Devonian rocks that lie in the footwall of the Lizard Complex preserve a record of the closure of the Rheic Ocean (Nance et al. 2010). A major period of extensional rifting was initiated during the middle Devonian (Bluck et al. 1988, 1992). East-west-trending normal faults downthrowing to the south separated marine shelf and fluvial basins in the north of Cornwall from the deep-water Gramscatho Basin to the south. The latter is dominated by the turbiditic sandstones and mudstones of the Gramscatho Group. The basin was filled from the south by turbidites derived from the erosion of advancing nappes (Floyd & Leveridge 1987). The turbidite successions include sedimentary mélanges of the Meneage Formation (Barnes 1983), which also contain blocks of MORB-type volcanics and mica schist as well as large (200 m) quartzite blocks with Ordovician faunas that are closely comparable with the Grès Armoricain of northwest France (Sadler 1974). Two granite pebbles within the Meneage Formation yielded U-Pb zircon lower intercept ages of  $373 \pm 6$  Ma and  $422 \pm 4$  Ma which were interpreted as protolith ages (Dorr et al. 1999). The upper intercept ages of  $2606 \pm 40$  Ma and  $2445 \pm 19$  Ma were thought to indicate the presence of an inherited Neoproterozoic or Palaeoproterozoic source terrane.

Together the data suggest derivation from a magmatic arc that developed on the leading edge of the Armorican plate (Dorr et al. 1999).

Two samples were analysed for the present study, both collected from the Meneage Formation north of Porthallow (Figs 3 & 4a). Sample LIZ 1 is a Devonian sandstone that forms the matrix of a debris-flow deposit (Fig 4c). Sample LIZ 3 is an exotic quartzite block (Fig 4b), part of the suite correlated by previous workers with the Ordovician Grès Armorican in Normandy.

### **Analytical techniques**

**Zircon preparation:** Zircon concentrates were separated at the Museum für Mineralogie und Geologie (Senckenberg Naturhistorische Sammlungen Dresden). Fresh 1 kg samples of sandstone were crushed and sieved and then a heavy mineral separate was concentrated by use of a heavy liquid (lithium heteropolytungstates in water). A final concentration was made by magnetic separation in a Frantz isodynamic separator. Selection of the zircon grains for U-Pb dating was achieved by hand-picking under a binocular microscope. All zircon grains are either rounded or sub-rounded. Zircon grains of all sizes and morphological types were selected for single grain analysis by LA-ICP-MS. Zircon crystals were set in synthetic resin mounts, polished to approximately half their thickness and cleaned in a warm dilute HNO<sub>3</sub> ultrasonic bath followed by rinsing in de-ionised water. Cathodoluminescence images of selected zircon grains are presented in Figure 5.

**LA-ICP-MS U-Pb dating:** U-Pb age determination of single grains was determined by LA-ICP-MS at the Natural History Museum, London using a New-Wave UP213 frequency quintupled solid-state Nd:YAG laser ( $\lambda=213$  nm) coupled to a PlasmaQuad 3 quadrupole ICP-MS. Samples and standard were placed in an airtight chamber which was flushed by helium gas carrying the ablated material to the ICP-MS, mixed with Ar prior to injection to the plasma torch. U-Pb and Pb-Pb ratios of the unknowns were determined relative to that of the 91500 zircon standard with certified ID-TIMS ages of  $1062.4 \pm 0.4$  Ma for  $^{206}\text{Pb}/^{238}\text{U}$  and  $1065.4 \pm 0.3$  Ma for  $^{207}\text{Pb}/^{206}\text{Pb}$  (Wiedenbeck et al. 1995). Collection of data spanned up to 180s per analysis and includes a gas background taken during the initial c. 60 s. To reduce the

extent of inter-element laser induced fractionation, the sample was moved relative to the laser beam along a line. The nominal diameter of the laser beam was 60 $\mu\text{m}$  for the standard and 30 $\mu\text{m}$  or 45 $\mu\text{m}$  for the unknowns. Pulse energy of the laser was 0.03-0.06 mJ per pulse for the unknowns and 0.09 mJ per pulse for the standards with an energy density of 3.5 J/cm<sup>2</sup> and a repetition rate of 20 Hz. Only well-preserved zones within individual grains were analysed (Figure 5), in order to escape metamorphic rims and altered domains. Further discussion of the analytical protocols used in this study can be found in Fernández-Suárez et al. (2002a) and Jeffries et al. (2003). Raw data reduction was performed using LAMTRACE, a macro based spreadsheet written by Simon Jackson (Macquarie University, Australia). Calculations and plotting of concordia diagrams were achieved using Isoplot/Ex rev. 2.49 (Ludwig 2001), probability density plots and histograms were prepared by AgeDisplay (Sircombe 2004). For grains younger than 1 Ga, the <sup>206</sup>Pb/<sup>238</sup>Pb age is quoted. For grains older than 1 Ga, the <sup>207</sup>Pb/<sup>206</sup>Pb age is used. Only grains concordant in the range 85 to 115% were used in the probability plots and histograms.

## Results

U-Pb data of detrital zircon grains are represented in the concordia, histograms, and binned frequency plots of figures 6 to 10 and in the supplementary data tables 1 to 5. The tables also contain information on litho- and biostratigraphy, sample location, and co-ordinates.

Sample ROC 1 is dominated by late Neoproterozoic grains (30 out of 48) that lie close to or on concordia and range in age from 547  $\pm$  8 Ma to 685  $\pm$  11 Ma (Fig 6). Of the remaining analyses, most are variably discordant. Thirteen yield Palaeoproterozoic ages with relative age peaks of c. 1850 and 2100 and 2400 Ma, four are Neoproterozoic, and the oldest grain is dated at 3113  $\pm$  31 Ma.

Sample AM 1 is dominated by late Neoproterozoic to early Cambrian grains (35 out of 40) that mostly lie close to or on concordia and range in age from 514  $\pm$  10 Ma to



627 ± 5 Ma (Fig 7). The remaining five analyses are somewhat discordant. Four Palaeoproterozoic grains yield ages of c. 1800 Ma(3), c. 2300 Ma(1), and the oldest grain is latest Neoproterozoic and dated at 2522 ± 15 Ma.

Sample AM 2 is dominated by late Neoproterozoic to middle Cambrian grains (27 out of 40) close to or on concordia and ranging in age from 515 ± 7 Ma to 695 ± 9 Ma (Fig 8). An older Neoproterozoic cluster features three concordant or slightly discordant analyses at c. 905-997 Ma. Of the remaining ten analyses, nine are Palaeoproterozoic with relative age peaks of c. 1800, 1850, 1900, 2000 and 2150 Ma, and the oldest grain is Neoproterozoic and dated at 2636 ± 35 Ma.

Sample LIZ 1 is dominated by late Neoproterozoic to late Cambrian grains (29 out of 54) close to or on concordia and ranging in age from 496 ± 22 Ma to 709 ± 18 Ma (Fig 9). Two Mesoproterozoic grains yield ages of c. 1028 and 1431 Ma. Of the remaining nineteen analyses, eighteen are Palaeoproterozoic with major relative age peaks at c. 2000 and 2100 Ma, and the oldest grain is Neoproterozoic and dated at 2593 ± 39 Ma.

Sample LIZ 3 is dominated by late Neoproterozoic to early Cambrian grains (37 out of 50) close to or on concordia and ranging in age from 531 ± 5 Ma to 646 ± 14 Ma (Fig 10). Two Mesoproterozoic grains yield ages of c. 1338 and 1485 Ma. Of the remaining eleven slightly discordant analyses, ten are Palaeoproterozoic with major relative age peaks at c. 2000 and 2100 Ma, and the oldest grain is Neoproterozoic and dated at 2641 ± 25 Ma.

## **Discussion and conclusions**

Detrital zircons analyzed from the three samples obtained from the Armorican Massif have a distinctive bimodal age distribution, dominated by late Neoproterozoic to middle Cambrian (c. 710-518 Ma) and Palaeoproterozoic (c. 1800-2200 Ma) groupings (Fig 11). Additionally, the samples contain minor amounts of Mesoproterozoic to early Neoproterozoic detritus. There has been much debate

surrounding what is a meaningful statistical population in detrital zircon analysis (e.g. Dodson et al. 1988; Sircombe 2000). According to Dodson et al. (1988), at least 59 randomly selected grains need to be measured to reduce the probability of missing a provenance component to 5%. In our study, we measured 60 grains per sample, 40-50 of which yielded analyses that were in the range of concordance of 85-115% and incorporated into data presentation and interpretation. Taking the three Armorican samples together (ROC 1, ARM 1 and ARM 2), this equates to 127 analyses, and the two Lizard samples (LIZ 1 and LIZ 2) provide a further 104 analyses. We are therefore confident that we have identified all major provenance components within the two sets of samples.

The samples have essentially the same bimodal age distribution as detrital zircons analyzed from other samples of the Brioverian Supergroup (Fernández-Suárez et al. 2002b; Samson et al. 2005). Both groupings can be readily linked with lithologies exposed within the Cadomian belt as well as the West African craton which is characterized by major tectonothermal events at 2.0 to 2.4 Ga (Fig 11). Similar detrital zircon age distributions are characteristic of Neoproterozoic successions in SW Iberia (Fernández-Suárez et al. 2002a) and, in particular, the Saxothuringian and Moldanubian zones in central Europe (Fig 11). On this basis, these crustal blocks are thought to have been located adjacent to the NW Africa segment of the Gondwanan margin during the Neoproterozoic and Lower Palaeozoic (Fernández-Suárez et al. 2002b; Samson et al. 2005).

The detrital zircon signature of Avalonia is quite distinct from that of Armorica in that there is a much larger proportion of Mesoproterozoic detritus (Fig 11; Collins & Buchan 2004; Murphy et al. 2004; Samson et al. 2005; Strachan et al. 2007). This contrasting signature is consistent with a location close to the Amazonian craton which records Mesoproterozoic tectonothermal activity at c. 1.6 and 1.1 Ga (Murphy et al. 2004; Collins & Buchan 2004; Samson et al. 2005; Strachan et al. 2007). Similar detrital zircon age distributions are characteristic of Neoproterozoic successions in NW Iberia (Fernández-Suárez et al. 2002b) and Bohemia (Friedl et al. 2000; Samson et al. 2005), and by implication these crustal blocks are also thought to have been located adjacent to Amazonia. It has been suggested that a major phase of Cambrian(?) sinistral strike-slip faulting displaced these crustal blocks along

the Gondwanan margin into a location between the West African craton and Armorica (Fernández-Suárez et al. 2002b).

The two samples taken from the Devonian Meneage Formation in the footwall of the Lizard ophiolite display an identical provenance to the three samples analysed from Armorica (Fig 11). This is consistent with: a) derivation of these mélangé deposits from the over-riding Armorican plate during closure of the Rheic Ocean, collision of Avalonia and Armorica, and obduction of the Lizard ophiolite (Fig 12; Holder & Leveridge 1986; Dörr et al. 1999), and b) correlation of the quartzite blocks within the Meneage Formation with the Ordovician Grès Armoricain Formation (Sadler 1974). The absence of identifiable clasts of Brioverian material in the Meneage Formation suggests that many of the detrital zircons are second cycle, derived from reworking of the Lower Palaeozoic cover to the basement of Armorica. We cannot absolutely preclude the incorporation of Avalonian material within the Meneage Formation, and further material needs to be analysed to provide a broader database. The presence of two Mesoproterozoic grains within sample LIZ 1 might be taken as indicative of at least partial derivation from an Avalonian source. However, sample LIZ 3 also contains two Mesoproterozoic grains but is more firmly linked to Armorica by the palaeontological evidence (Sadler 1974).

Our dataset is therefore consistent with the south-directed subduction geometry of the Rheic collision zone invoked by Holder & Leveridge (1986) (Fig 12). Such a geometry would be expected to have resulted in generation of a magmatic arc on the over-riding Armorican plate, consistent with the Silurian-Devonian U-Pb zircon ages obtained from granite pebbles in the Meneage Formation by Dörr et al. (1999). However, our new dataset does not contain any evidence for detrital zircons of this age. Detrital zircons analysed from the matrix of the Meneage Formation therefore only provide a partial picture of the composition of the over-riding Armorican plate in the vicinity of the Rheic suture.

### **Acknowledgments**

The authors acknowledge discussion in the field with participants of the IGCP 497 fieldtrip to SW England in July 2005, and reviews from James Braid and Nigel Woodcock that improved the paper.



## References

- Ballevre M, Bosse V, Ducassou C, Pitra P (2009) Palaeozoic history of the Armorican Massif: Models for the tectonic evolution of the suture zones. *C.R. de Geosci* 341: 174-201.
- Barnes RP (1983) The stratigraphy of a sedimentary melange and associated deposits in South Cornwall, England. *Proc. Geol Assoc* 94: 217-229.
- Barnes RP, Andrews JR (1984) Hot or cold emplacement of the Lizard Complex? *J Geol Soc Lond* 141: 37-39.
- Barnes, R.P. & Andrews, J.R. 1986. Upper Palaeozoic ophiolite generation and obduction in south Cornwall. *J Geol Soc Lond* 143,117-124.
- Bertrand L (1921) *Les anciennes mers de la France et leur deposits*. Flammarion, Paris.
- BIRPS & ECORS (1986) Deep seismic reflection profiling between England, France and Ireland. *J Geol Soc Lond* 143: 45-52.
- Bluck BJ, Haughton PDW, House MR, Selwood EB, Tunbridge IP (1988) Devonian of England, Wales and Scotland. In: McMillan NJ, Embry AF, Glass DJ (eds) *Devonian of the World*. *Mem Canad Soc Petrol Geol* 14: 305-324.
- Bluck BJ, Cope JCW, Scrutton CT (1992) Devonian. In: Cope JCW, Ingham JK, Rawson, PF (eds) *Atlas of Palaeogeography and Lithofacies*. *Geol Soc, Lond*, 57-66.
- Bromley AV (1979) Ophiolitic origin of the Lizard Complex. *J Camborne School of Mines* 79: 25-38.
- Calvez JY, Vidal P (1978) Two billion years old relicts in the Hercynian belt of Western Europe. *Contribs Min & Pet* 65: 395-399.
- Cawood PA, Nemchin AA, Smith M, Loewy S (2003) Source of the Dalradian Supergroup constrained by U-Pb dating of detrital zircon and implications for the East Laurentian margin. *J Geol Soc Lond* 160: 231-246.
- Cawood PA, Nemchin AA, Strachan RA, Kinny PD, Loewy S (2004) Laurentian provenance and tectonic setting for the upper Moine Supergroup, Scotland, constrained by detrital zircons from the Loch Eil and Glen Urquhart successions. *J Geol Soc Lond* 161: 863-874.
- Cawood PA, Nemchin AA, Strachan RA, Prave AR, Krabbendam M (2007) Sedimentary basin and detrital zircon record along East Laurentia and Baltica during assembly and breakup of Rodinia. *J Geol Soc Lond* 164: 257-275.

- Chantraine J, Auvray B, Rabu D (1994) The Cadomian Orogeny in the Armorican Massif: Igneous Activity. In: Keppie JD (ed) Pre-Mesozoic Geology in France. Springer, Berlin, 111-125.
- Chen Y, Clark AH, Farrar E, Wasteneys HAHP, Hodgson MJ, Bromley AV (1993) Diachronous and independent histories of plutonism and mineralization in the Cornubian Batholith, southwest England. *J Geol Soc Lond* 150: 1183-1191.
- Chesley JT, Halliday AN, Snee LWE, Mezger K, Shepherd TJ, Scrivener RC (1993) Thermochronology of the Cornubian batholith in southwest England: implications for pluton emplacement and protracted hydrothermal mineralization. *Geochim Cosmo Acta* 57: 1817-1835.
- Clark AH, Scott DJ, Sandemann HA, Bromley AV (1998) Siegenian generation of the Lizard ophiolite: U-Pb zircon age data for plagiogranite, Porthkerris, Cornwall. *J Geol Soc Lond* 155: 595-598.
- Cocks LRM, Torsvik TH (2002) Earth geography from 500 to 400 million years ago: A faunal and palaeomagnetic review. *J Geol Soc Lond* 159: 631-644.
- Cogné J (1990) The Cadomian orogeny and its influence on the Variscan evolution of western Europe. In: D'Lemos RS, Strachan RA, Topley CG (eds) The Cadomian Orogeny. *Geol Soc Lond, Spec Pub* 51: 305-311.
- Collins AS, Buchan C (2004) Provenance and age constraints of the South Stack Group, Anglesey, UK: U-Pb SIMS detrital zircon data. *J Geol Soc Lond* 161: 743-746.
- Coward MP, McClay KR (1983) Thrust tectonics of S. Devon. *J Geol Soc Lond* 140: 215-228.
- Dodson MH, Compston W, Williams IS, Wilson JF (1988) A search for ancient detrital zircons in Zimbabwean sediments. *J Geol Soc Lond* 145: 977-983.
- Doré F (1994) Cambrian of the Armorican Massif. In: Keppie JD (ed) Pre-Mesozoic Geology in France. Springer, Berlin, 136-141.
- Dörr W, Floyd PA, Leveridge BE (1999) U-Pb ages and geochemistry of granite pebbles from the Devonian Menaver Conglomerate, Lizard peninsula: provenance of Rhenohercynian flysch of SW England. *Sed Geol* 124: 131-147.
- Drost K, Gerdes A, Jeffries T, Linnemann U, Storey C (2011) Provenance of Neoproterozoic and early Palaeozoic siliciclastic rocks of the Teplá-Barrandian unit (Bohemian Massif): Evidence from U-Pb detrital zircon ages. *Gondwana Res* 19: 213-231.
- Egal E, Guerrot C, Le Goff E, Thieblemont D, and Chantraine J (1996) The Cadomian Orogen revisited in North Brittany. In: Nance RD, Thompson MD (eds) Avalonian and

Related Peri-Gondwanan Terranes of the Circum-Atlantic. *Geol Soc Am, Spec Pap*, 304: 281-318.

Fernández-Suárez J, Gutiérrez-Alonso G, Cox R, Jenner GA (2002a) Assembly of the Armorica Microplate: a strike-slip terrane delivery? Evidence from U-Pb ages of detrital zircons. *J Geol* 110: 619-626.

Fernández-Suárez J, Gutiérrez-Alonso G, Jeffries TE (2002b) The importance of along-margin terrane transport in northern Gondwana: insights from detrital zircon parentage in Neoproterozoic rocks from Iberia and Brittany. *Earth & Planet Sci Lett* 204: 75-88.

Floyd PA (1984) Geochemical characteristics and comparison of the basic rocks of the Lizard Complex and the basaltic lavas within the Hercynian troughs of SW England. *J Geol Soc Lond* 144: 531-542.

Floyd PA, Leveridge BE (1987) Tectonic environment of the Devonian Gramscatho basin, south Cornwall: framework mode and geochemical evidence from turbiditic sandstones. *J Geol Soc Lond* 144: 531-542.

Friedl G, Finger F, McNaughton NJ, Fletcher IR (2000) Deducing the ancestry of terranes: SHRIMP evidence for South America-derived Gondwana fragments in central Europe. *Geology* 28: 1035-1038.

Gibbons W, Thompson L (1991) Ophiolitic mylonites in the Lizard Complex: ductile extension in the lower crust. *Geology* 19: 1009-1012.

Hartley AJ (1993) Silesian sedimentation in southwest Britain: sedimentary responses to the developing Variscan orogeny. In: Gayer R, Greiling RO, Vogel AK (eds) *Rhenohercynian and Subvariscan Fold Belts*. Vieweg, Weisbaden/Braunschweig, 160-196.

Holder MT, Leveridge BE (1986) A model for the tectonic evolution of south Cornwall. *J Geol Soc Lond* 143: 125-134.

Jeffries TE, Fernández-Suárez J, Corfu F, Gutiérrez-Alonso G (2003) Advances in U-Pb geochronology using frequency quintupled Nd:YAG based laser ablation system and quadrupole based ICP-MS. *J Anal Atomic Spect* 18: 847-855.

Keppie JD, Nance RD, Murphy JB, Dostal J (2003) Tethyan, Mediterranean and Pacific analogues for the Neoproterozoic-Palaeozoic birth and development of peri-Gondwanan terranes and their transfer to Laurentia and Laurussia. *Tectonophysics* 365: 195-219.

Le Gall B (1990) Evidence of an imbricate thrust belt in the southern British Variscides: contributions of South-Western approaches traverse (SWAT) deep



seismic reflection profiling recorded through the English Channel. *Tectonics* 9: 283-302.

Leveridge BE, Holder MT, Day GA (1984) Thrust nappe tectonics in the Devonian of south Cornwall and the western English Channel. In: Hutton DHW, Sanderson DJ (eds) *Variscan Tectonics of the North Atlantic Region*. Geol Soc Lond, Spec Pub 14: 103-112.

Linnemann U, McNaughton NJ, Romer RL, Gehmlich M, Drost K, Tonk C (2004) West African provenance for Saxo-Thuringia (Bohemian Massif): Did Armorica ever leave pre-Pangaeian Gondwana?-U-Pb SHRIMP zircon evidence and the Nd-isotopic record. *Int J Earth Sci* 93: 683-705.

Linnemann U, D'Lemos RS, Drost K, Jeffries T, Gerdes A, Romer RL, Samson SD, Strachan RA (2008) Cadomian tectonics. In: McCann T (ed) *The Geology of Central Europe, Volume 1: Precambrian and Palaeozoic*. Geol Soc Lond 103-154.

Ludwig KR (2001) *SQUID 1.00: A User's Manual*. Berkeley Geochronology Centre Special Publication 2, 19pp.

Matte P (1986) Tectonics and plate tectonic models for the Variscan belt of Europe. *Tectonophysics* 126: 329-374.

Murphy JB, Nance RD (1989) Model for the evolution of the Avalonian-Cadomian belt. *Geology* 17: 735-738.

Murphy JB, Nance RD (1991) Supercontinent model for the contrasting character of Late Proterozoic orogenic belts. *Geology* 19: 469-472.

Murphy JB, Strachan RA, Nance RD, Parker KD, Fowler MB (2000) Proto-Avalonia: a 1.2-1.0 Ga tectonothermal event and constraints for the evolution of Rodinia. *Geology* 29: 1071-1074.

Murphy JB, Fernández-Suárez J, Jeffries TE, Strachan RA (2004) U-Pb (LA-ICP-MS) dating of detrital zircons from Cambrian clastic rocks in Avalonia: erosion of a Neoproterozoic arc along the northern Gondwanan margin. *J Geol Soc Lond* 161: 243-254.

Nance RD, Murphy JB, Strachan RA, D'Lemos RS, Taylor GK (1991) Late Proterozoic tectonostratigraphic evolution of the Avalonian and Cadomian terranes. *Precam Res* 53: 41-78.

Nance RD, Murphy JB, Keppie JD (2002) Cordilleran model for the evolution of Avalonia. *Tectonophysics* 352: 11-31.

Nance RD, Murphy JB, Strachan RA, Keppie JD, Gutiérrez-Alonso G, Fernández-Suárez J, Quesada C, Linnemann U, D'Lemos RS, Pisarevsky SA (2007) Neoproterozoic-early

Palaeozoic tectonostratigraphy and palaeogeography of the peri-Gondwanan terranes: Amazonian versus West African connections. In: Nasser E, Liégeois J-P (eds) *The Boundaries of the West African Craton*. Geol Soc Lond, Spec Pub 297: 345-383.

Nance RD, Gutiérrez-Alonso G, Keppie JD, Linnemann U, Murphy, JB, Quesada C, Strachan RA, Woodcock, N.H. (2010) Evolution of the Rheic Ocean. *Gondwana Res*, 17: 194-222.

Pickering KT, Bassett MG, Siveter DJ (1988) Late Ordovician-Early Silurian destruction of the Iapetus Ocean: Newfoundland, British Isles and Scandinavia – a discussion. *Trans Roy Soc Edin Earth Sci* 79: 361-382.

Rabu D, Chantaine J, Chauvel JJ, Denis E, Balé P, Bardy Ph (1990) The Brioverian (Upper Proterozoic) and the Cadomian orogeny in the Armorican Massif. In: D'Lemos RS, Strachan RA, Topley CG (eds) *The Cadomian Orogeny*. Geol Soc Lond, Spec Pub 51: 81-94.

Rainbird RH, Hamilton MA, Young GM (2001) Detrital zircon geochronology and provenance of the Torridonian, NW Scotland. *J Geol Soc Lond* 158: 15-27.

Robardet M, Bonjour JL, Paris F, Morzadec P, Racheboeuf PR (1994) In: Keppie JD (ed) *Pre-Mesozoic Geology in France*. Springer, Berlin, 142-151.

Roberts S, Andrews JR, Bull JM, Sanderson DJ (1993) Slow-spreading ridge-axis tectonics: evidence from the Lizard Complex, UK. *Earth & Planet Sci Lett* 116: 101-112.

Sadler PM (1974) Trilobites from the Gorran quartzites, Ordovician of south Cornwall. *Palaeontology* 17: 71-93.

Samson SD, D'Lemos RS (1998) U-Pb geochronology and Sm-Nd isotopic composition of Proterozoic gneisses, Channel Islands, UK. *J Geol Soc Lond* 155: 609-618.

Samson SD, D'Lemos RS, Miller BV, Hamilton MA (2005) Neoproterozoic palaeogeography of the Cadomia and Avalon terranes: constraints from detrital zircon U-Pb ages. *J Geol Soc Lond* 162: 65-71.

Sanderson DJ (1984) Structural variations across the northern margin of the Variscides in NW Europe. In: Hutton DHW, Sanderson DJ (eds) *Variscan Tectonics of the North Atlantic Region*. Geol Soc Lond, Spec Pub 14: 149-165.

Seago RD, Chapman TJ (1988) The confrontation of structural styles and the evolution of a foreland basin in central SW England. *J Geol Soc Lond* 145: 789-800.

Shackleton RM, Ries AC, Coward MP (1982) An interpretation of the Variscan structures in SW England. *J Geol Soc Lond* 139: 533-541.

Sircombe KN (2000) Quantitative comparison of geochronological data using multivariate analysis: a provenance study example from Australia. *Geochim Cosmochim Acta* 64: 1593-1619.

Sircombe KN (2004) AgeDisplay: an EXCEL workbook to evaluate and display univariate geochronological data using binned frequency histograms and probability density distributions. *Computers & Geosci* 30: 21-31.

Soper NJ, Strachan RA, Holdsworth RE, Gayer RA, Greiling RO (1992) Sinistral transpression and the Silurian closure of Iapetus. *J Geol Soc Lond* 14:, 871-880.

Stampfli GM, Borel GD (2002) A plate tectonic model for the Palaeozoic and Mesozoic constrained by dynamic plate boundaries and restored synthetic oceanic isochrones. *Earth & Planet Sci Lett* 196: 17-33.

Strachan RA, D'Lemos RS, Dallmeyer RD (1996) Neoproterozoic evolution of an active plate margin: North Armorican Massif, France. In: Nance RD, Thompson MD (eds) *Avalonian and Related Peri-Gondwanan Terranes of the Circum-Atlantic*. *Geol Soc Am, Spec Pap* 304: 319-332.

Strachan RA, Collins AS, Buchan C, Nance RD, Murphy JB, D'Lemos RS (2007) Terrane analysis along a Neoproterozoic active margin of Gondwana: insights from U-Pb zircon geochronology. *J Geol Soc Lond* 164: 57-60.

Styles MT, Kirby GA (1980) New investigation of the Lizard Complex, Cornwall, and discussion of an ophiolite model. In: Panayiotou A (ed) *Ophiolites: Proceedings of the International Ophiolite Symposium, Cyprus, 1979*. Geological Survey Department, Nicosia, Cyprus, 517-526.

Taylor GK, Strachan RA (1990) Palaeomagnetism and tectonic models for Avalonian-Cadomian geology of the North Atlantic. In: Strachan RA, Taylor GK (eds) *Avalonian-Cadomian geology of the North Atlantic*. Blackie, Glasgow, 237-247.

Van Staal CR, Dewey JF, MacNiocaill C, McKerrow WS (1998) The Cambrian-Silurian tectonic evolution of the Northern Appalachians and British Caledonides: History of a complex west and southwest Pacific-type segment of Iapetus. In: Blundell D, Scott AC (eds) *Lyell: The present is the key to the past*. *Geol Soc Lond, Spec Pub* 143: 199-242.

Vearncombe JR (1980) The Lizard ophiolite and two phases of sub-oceanic deformation. In: Panayiotou A (ed) *Ophiolites: Proceedings of the International Ophiolite Symposium, Cyprus, 1979*. Geological Survey Department, Nicosia, Cyprus, 527-537.

Wiedenbeck M, Allé P, Corfu F, Griffin WL, Meier M, Oberli F, von Quadt A, Roddick JC, Spiegel W (1995) Three natural zircon standard for U-Th-Pb, Lu-Hf, trace element and REE analyses. *Geostand Newsletter*, 19: 1-23.



## Figure captions

Figure 1. Geological map of the Central European Variscides (modified from Ballèvre et al. 2009).

Figure 2. Generalized geological map of the North Armorican Massif (modified from Linnemann et al. 2008) and sample locations (ROC 1, AM 1, AM 2). Abbreviations: FSZ, Fresnaye shear zone; PCSZ, Plouer-Cancale shear zone. Inset shows the North Armorican shear zone (NASZ) and South Armorican shear zone (SASZ). Other abbreviations: C, Coutances; GM, Guingamp migmatites; NTB, North Trégor Batholith; PC, Penthièvre Complex; PP, Plourivo-Plouézec; SGG, Saint Germain le-Gaillard.

Figure 3. Generalized map of the Lizard area and sample locations (LIZ 1, LIZ 3) (modified from Barnes & Andrews 1986).

Figure 4. Photographs from the sampling site in the Lizard area (samples LIZ 1 and LIZ 3, Menage Formation, Gramscatho Group, Devonian, see also Fig. 3). A – Menage Formation and olistolith of a Lower Ordovician quartzite (Nare Cove, c. 1.3 km N of Porthallow), B – Olistolith of the Lower Ordovician quartzite, sample LIZ 3), C – Mélange deposit of the Meneage formation, sample LIZ 1 was taken from the sandstone matrix).

Figure 5. Cathodoluminescence images of selected zircon grains from samples ROC 1, LIZ1, and LIZ 3. For grains younger than 1 Ga, the  $^{206}\text{Pb}/^{238}\text{Pb}$  age is quoted. For grains older than 1 Ga, the  $^{207}\text{Pb}/^{206}\text{Pb}$  age is used.

Figure 6. U-Pb ages of detrital zircon grains from sample ROC 1 (graywacke, Upper Brioverian, Post-Bedded Chert Brioverian, Ediacaran, Rocreux near Bretteville s. Laize, Normandy, Armorican Massif). Concordia diagram (A) and combined binned



frequency and probability density distribution plots of detrital zircon grains in the range of 400 to 3200 Ma (B) and of 400 to 800 Ma (C).

Figure 7. U-Pb ages of detrital zircon grains from sample AM 1 (sandstone, Lower Cambrian, Le Rozel formation, Le Rozel, Normandy, Armorican Massif). Concordia diagram (A) and combined binned frequency and probability density distribution plots of detrital zircon grains in the range of 400 to 2900 Ma (B) and of 400 to 1100 Ma (C).

Figure 8. U-Pb ages of detrital zircon grains from sample AM 2 (quartzite, Lower Ordovician (Arenigian), Armorican quartzite formation, Les Rieux, Normandy, Armorican Massif). Concordia diagram (A) and combined binned frequency and probability density distribution plots of detrital zircon grains in the range of 400 to 3000 Ma (B) and of 400 to 1100 Ma (C).

Figure 9. U-Pb ages of detrital zircon grains from sample LIZ 1 (greywacke matrix of the *mélange* deposit, Devonian, Meneage Formation, Gramscatho Group, Nare Cove, c. 1.3 km north of Porthallow, Cornwall, UK). Concordia diagram (A) and combined binned frequency and probability density distribution plots of detrital zircon grains in the range of 400 to 3000 Ma (B) and of 400 to 1100 Ma (C).

Figure 10. U-Pb ages of detrital zircon grains from sample LIZ 3 (quartzite olistolith correlated with the Armorican quartzite in the *mélange* deposit of the Devonian Meneage Formation, Gramscatho Group, Nare Cove, c. 1.3 km north of Porthallow, Cornwall, UK) (see also Figure 4). Concordia diagram (A) and combined binned frequency and probability density distribution plots of detrital zircon grains in the range of 400 to 3000 Ma (B) and of 400 to 800 Ma (C).

Figure 11. Detrital zircon age distributions the samples studied in this paper together with zircon age distributions of Baltica, Amazonia, East Avalonia (Brabant massif), Armorica (Cadomian basement in the Saxo-Thuringian and Moldanubian zones, Bohemian Massif), and the West African craton (data compilation from Drost et al.

2011; Linnemann et al. 2004, 2008). Note the general occurrence of Mesoproterozoic zircon ages in Baltica, Amazonia, and Avalonia and the contrasting rarity of the same zircon populations in Armorica (Cadomia) and the West African craton.

Figure 12. A model for the Devonian tectonic evolution of the Lizard ophiolite complex in South Cornwall, depicting the progressive erosion of advancing thrust nappes of the Armorican plate (right) onto the southern margin of Avalonia (left) (from Holder & Leveridge 1986). Cne-Carne Formation, Ds-Dartmouth Slates, Mg-Meadfoot Group, Ms-Mylor Slate Formation, Pd-Pendower Formation, Pto-Portscatho Formation, Ptn-Porthtowan Formation, Rbr-Roseland Breccia Formation. Tectonic units: Ck-Carrick Nappe, CT-Carrick Thrust, DP-Dodman Nappe, DT-Dodman Thrust, LT-Lizard Thrust, Lz-Lizard Nappe, N-Normannian Nappe, NT-Normannian Thrust.

Table 1: LA-ICP-MS detrital zircon data of sample ROC 1, n = 48/60, concordant in the range of 85-115%, greywacke turbidite from the Upper Brioverian (Post-Bedded Chert Brioverian), Bocaine Zone, Rocreux near Bretteville s. Laize, Normandy, France, (sample location: road cut at Rocreux in the valley of the Laize river, co-ordinates: 49°03'16.03" N, 0°20'41.28" W).

spot	grain	206/238	err	207/235	err	207/206	err	Age206/238	2 $\sigma$	Age207/235	2 $\sigma$	Age207/206	2 $\sigma$	conc%
mr24h09	ROC1 41	0.08850	0.00070	0.72190	0.01011	0.05914	0.00100	547	8	552	12	572	74	96
mr24g07	ROC1 27	0.09030	0.00062	0.72920	0.00620	0.05856	0.00042	557	7	556	7	550	32	101
mr24e13	ROC1 09	0.09080	0.00066	0.72480	0.01348	0.05791	0.00119	560	8	554	16	526	90	106
mr24k08	ROC1 52	0.09110	0.00055	0.76060	0.00578	0.06051	0.00042	562	6	574	7	622	30	90
mr24f05	ROC1 13	0.09160	0.00059	0.72960	0.00883	0.05776	0.00077	565	7	556	10	520	58	109
mr24h11	ROC1 43	0.09200	0.00063	0.73330	0.01085	0.05779	0.00091	567	7	558	13	520	68	109
mr24f08	ROC1 16	0.09220	0.00069	0.76690	0.00759	0.06029	0.00037	569	8	578	9	612	26	93
mr24k14	ROC1 58	0.09280	0.00073	0.76530	0.00574	0.05977	0.00057	572	9	577	7	594	42	96
mr24k15	ROC1 59	0.09290	0.00051	0.76370	0.00672	0.05958	0.00046	573	6	576	8	588	34	97
mr24f13	ROC1 21	0.09320	0.00072	0.76620	0.00766	0.05960	0.00069	575	9	578	9	588	52	98
mr24f11	ROC1 19	0.09350	0.00071	0.73680	0.00936	0.05717	0.00065	576	8	561	11	498	50	116
mr24e16	ROC1 12	0.09370	0.00124	0.78500	0.01256	0.06078	0.00055	577	15	588	14	630	40	92
mr24e07	ROC1 03	0.09440	0.00048	0.80910	0.00744	0.06213	0.00066	582	6	602	8	678	46	86
mr24e08	ROC1 04	0.09500	0.00085	0.77010	0.00901	0.05878	0.00045	585	10	580	10	558	32	105
mr24g14	ROC1 34	0.09510	0.00078	0.77060	0.00709	0.05875	0.00052	586	9	580	8	556	38	105
mr24f09	ROC1 17	0.09530	0.00055	0.77960	0.00686	0.05935	0.00049	587	7	585	8	578	36	102
mr24g08	ROC1 28	0.09590	0.00081	0.79630	0.00764	0.06020	0.00034	590	9	595	9	610	24	97
mr24k12	ROC1 56	0.09600	0.00122	0.78170	0.01610	0.05902	0.00133	591	14	586	18	566	100	104
mr24k07	ROC1 51	0.09630	0.00120	0.79650	0.01027	0.05999	0.00079	592	14	595	12	602	56	98
mr24e14	ROC1 10	0.09680	0.00102	0.82690	0.01125	0.06193	0.00048	596	12	612	13	670	34	89
mr24g10	ROC1 30	0.09880	0.00075	0.81750	0.00891	0.06002	0.00053	607	9	607	10	604	38	100
mr24h05	ROC1 37	0.09950	0.00086	0.83410	0.00859	0.06079	0.00075	611	10	616	9	630	52	97
mr24h13	ROC1 45	0.10030	0.00090	0.83620	0.00828	0.06045	0.00073	616	11	617	9	618	52	100
mr24h10	ROC1 42	0.10080	0.00065	0.84920	0.00977	0.06109	0.00063	619	8	624	11	642	44	96



mr24h06	ROC1 38	0.10110	0.00086	0.85570	0.00625	0.06139	0.00041	621	10	628	7	652	28	95
mr24k05	ROC1 49	0.10150	0.00066	0.85330	0.00700	0.06098	0.00035	623	8	626	8	638	24	98
mr24g06	ROC1 26	0.10320	0.00090	0.87950	0.00774	0.06181	0.00041	633	10	641	8	666	28	95
mr24g09	ROC1 29	0.10400	0.00063	0.85110	0.02247	0.05933	0.00160	638	7	625	25	578	118	110
mr24g12	ROC1 32	0.10850	0.00100	0.91260	0.01342	0.06097	0.00098	664	12	658	14	638	70	104
mr24e06	ROC1 02	0.10870	0.00096	0.92580	0.01120	0.06175	0.00054	665	11	665	12	664	38	100
mr24f16	ROC1 24	0.11220	0.00096	0.93560	0.01927	0.06049	0.00142	685	11	671	20	620	102	110
mr24h15	ROC1 47	0.32290	0.00165	5.19900	0.03171	0.11676	0.00077	1804	16	1852	10	1906	24	95
mr24k16	ROC1 60	0.32830	0.00230	5.69070	0.05065	0.12569	0.00057	1830	22	1930	15	2038	16	90
mr24f14	ROC1 22	0.33170	0.00226	5.28300	0.03381	0.11550	0.00069	1847	22	1866	11	1886	22	98
mr24h16	ROC1 48	0.33610	0.00192	5.76650	0.03402	0.12440	0.00049	1868	19	1941	10	2020	14	92
mr24f15	ROC1 23	0.33660	0.00293	5.27860	0.06229	0.11372	0.00156	1870	28	1865	20	1858	50	101
mr24k06	ROC1 50	0.37000	0.00185	6.49950	0.02795	0.12739	0.00059	2029	17	2046	7	2062	16	98
mr24e12	ROC1 08	0.37550	0.00308	6.77600	0.04608	0.13084	0.00079	2055	29	2083	12	2108	20	97
mr24h08	ROC1 40	0.38180	0.00191	6.74800	0.04184	0.12814	0.00041	2085	18	2079	11	2072	12	101
mr24f06	ROC1 14	0.38900	0.00233	7.10970	0.06043	0.13252	0.00091	2118	22	2125	15	2130	24	99
mr24e05	ROC1 01	0.43810	0.00215	10.24630	0.06148	0.16958	0.00078	2342	19	2457	11	2552	16	92
mr24k11	ROC1 55	0.45130	0.00420	10.75860	0.10543	0.17287	0.00109	2401	37	2502	18	2584	22	93
mr24h14	ROC1 46	0.49920	0.00180	14.28570	0.05571	0.20753	0.00114	2610	15	2769	7	2886	18	90
mr24e10	ROC1 06	0.51990	0.00452	13.14520	0.10385	0.18333	0.00055	2699	38	2690	15	2682	10	101
mr24h07	ROC1 39	0.54420	0.00332	16.15720	0.10664	0.21530	0.00086	2801	28	2886	13	2944	14	95
mr24f10	ROC1 18	0.55130	0.00402	15.15010	0.11666	0.19927	0.00145	2831	33	2825	15	2820	24	100
mr24g15	ROC1 35	0.62090	0.00385	21.50850	0.15916	0.25120	0.00103	3113	31	3162	14	3192	14	98



Table 2: LA-ICP-MS detrital zircon data for sample AM1, n = 40/60, concordant in the range of 85-115%, concordant from the Le Rozel Formation, Lower Cambrian, Normandy, Armorican Massif, France (sample location: beach south of Le Rozel, co-ordinates: 49°28'46" N, 01°50'39" W).

spot	grain	206/238	err	207/235	err	207/206	err	Age206/238	2 $\sigma$	Age207/235	2 $\sigma$	Age207/206	2 $\sigma$	conc%
mr18b16	AM1-48	0.08310	0.0008	0.6821	0.00539	0.05953	0.00054	514	10	528	8	586	11	88
mr18c08	AM1-52	0.08420	0.0006	0.6800	0.00700	0.05855	0.00054	521	7	527	11	550	10	95
mr18c11	AM1-55	0.08460	0.0003	0.6871	0.00467	0.05891	0.00043	523	4	531	7	562	8	93
mr17g06	AM1-2	0.08610	0.0004	0.6904	0.00545	0.05816	0.00054	532	5	533	8	534	10	100
mr18b13	AM1-45	0.08620	0.0007	0.7109	0.00768	0.05980	0.00070	533	8	545	12	596	14	89
mr18a05	AM1-25	0.08630	0.0006	0.7089	0.00595	0.05955	0.00038	534	7	544	9	586	7	91
mr17g05	AM1-1	0.08680	0.0004	0.7026	0.00499	0.05870	0.00047	537	4	540	8	554	9	97
mr18a11	AM1-31	0.08700	0.0004	0.7116	0.00626	0.05927	0.00040	538	5	546	10	576	8	93
mr18b10	AM1-42	0.08700	0.0003	0.7225	0.00506	0.06023	0.00039	538	3	552	8	610	8	88
mr17h09	AM1-17	0.08710	0.0006	0.7224	0.00592	0.06011	0.00045	539	7	552	9	606	9	89
mr18c14	AM1-58	0.08740	0.0006	0.7075	0.00849	0.05872	0.00063	540	7	543	13	556	12	97
mr17h07	AM1-15	0.08800	0.0004	0.6896	0.00531	0.05679	0.00041	544	5	533	8	482	7	113
mr17g10	AM1-6	0.08820	0.0006	0.7099	0.00738	0.05839	0.00076	545	7	545	11	544	14	100
mr18b14	AM1-46	0.08880	0.0003	0.7378	0.00494	0.06025	0.00043	548	4	561	8	612	9	90
mr18c07	AM1-51	0.08880	0.0003	0.7249	0.00457	0.05920	0.00028	548	4	554	7	574	5	95
mr18b06	AM1-38	0.08890	0.0005	0.7276	0.00466	0.05937	0.00042	549	6	555	7	580	8	95
mr17h14	AM1-22	0.08910	0.0006	0.7116	0.00726	0.05793	0.00039	550	7	546	11	526	7	105
mr18a12	AM1-32	0.08910	0.0005	0.7138	0.00450	0.05808	0.00054	550	6	547	7	532	10	103
mr18a13	AM1-33	0.08930	0.0009	0.7466	0.01127	0.06065	0.00081	551	11	566	17	626	17	88
mr18b11	AM1-43	0.08920	0.0005	0.7230	0.00636	0.05880	0.00047	551	6	552	10	558	9	99
mr17h15	AM1-23	0.08930	0.0004	0.7031	0.00464	0.05707	0.00037	552	5	541	7	494	6	112
mr17g07	AM1-3	0.08970	0.0006	0.7270	0.00654	0.05877	0.00049	554	7	555	10	558	9	99
mr17h06	AM1-14	0.09000	0.0004	0.7402	0.00496	0.05965	0.00042	555	5	563	8	590	8	94

mr18a06	AM1-26	0.08990	0.0003	0.7382	0.00384	0.05954	0.00031	555	4	561	6	586	6	95
mr17h11	AM1-19	0.09020	0.0006	0.7233	0.00383	0.05816	0.00028	557	7	553	5	534	5	104
mr17g11	AM1-7	0.09080	0.0004	0.7415	0.00482	0.05925	0.00034	560	5	563	7	576	7	97
mr17h10	AM1-18	0.09110	0.0007	0.7756	0.00884	0.06174	0.00041	562	9	583	13	664	9	85
mr18b05	AM1-37	0.09220	0.0004	0.7558	0.00431	0.05944	0.00032	569	4	572	6	582	6	98
mr18b12	AM1-44	0.09270	0.0004	0.7694	0.00354	0.06018	0.00033	571	5	579	7	610	7	94
mr18b07	AM1-39	0.09290	0.0008	0.7858	0.01116	0.06136	0.00075	572	10	589	17	650	16	88
mr17g14	AM1-10	0.09290	0.0006	0.7714	0.00586	0.06022	0.00031	573	7	581	9	610	6	94
mr18a09	AM1-29	0.09370	0.0004	0.7649	0.00283	0.05918	0.00021	578	4	577	4	572	4	101
mr18a10	AM1-30	0.09450	0.0003	0.7924	0.00428	0.06077	0.00030	582	4	593	6	630	6	92
mr18c16	AM1-60	0.09480	0.0004	0.7806	0.00500	0.05973	0.00036	584	5	586	8	592	7	99
mr18a07	AM1-27	0.10220	0.0004	0.8767	0.00473	0.06220	0.00027	627	5	639	7	680	6	92
mr17g13	AM1-9	0.31510	0.0017	5.3598	0.02733	0.12334	0.00030	1766	19	1878	19	2004	10	88
mr17h05	AM1-13	0.32510	0.0019	5.2425	0.03827	0.11694	0.00106	1814	21	1860	27	1908	35	95
mr17h12	AM1-20	0.33070	0.0017	5.2541	0.03625	0.11520	0.00065	1842	18	1861	26	1882	21	98
mr18b08	AM1-40	0.42570	0.0023	9.2282	0.05352	0.15719	0.00041	2286	25	2361	27	2424	13	94
mr17g16	AM1-12	0.47880	0.0014	12.2659	0.03066	0.18577	0.00046	2522	15	2625	13	2704	14	93



Table 3: LA-ICP-MS detrital zircon data for sample AM2, n = 39/60, concordant in the range of 85-115%, quartzite from the Armorican Quartzite Formation, Lower Ordovician (Arenig), Normandy, Armorican Massif, France (sample location: c. 2 km SW of the city of Les Pieux; co-ordinates: 49°30'26" N, 1°50'21" W).

spot	grain	206/238	err	207/235	err	207/206	err	Age206/238	2 $\sigma$	Age207/235	2 $\sigma$	Age207/206	2 $\sigma$	conc%
mr17f05	AM2-49	0.08320	0.00058	0.67430	0.00418	0.058800	0.000329	515	7	523	6	558	6.2	92
mr17f13	AM2-57	0.08400	0.00060	0.68390	0.01265	0.059010	0.000974	520	7	529	20	566	18.7	92
mr17c16	AM2-24	0.08440	0.00104	0.67820	0.00732	0.058240	0.000641	523	13	526	11	538	11.8	97
mr17f06	AM2-50	0.08630	0.00040	0.69280	0.00478	0.058230	0.000466	533	5	534	7	538	8.6	99
mr17f16	AM2-60	0.08660	0.00062	0.69610	0.00912	0.058290	0.000816	535	8	536	14	540	15.1	99
mr17d13	AM2-33	0.08690	0.00061	0.70290	0.00907	0.058650	0.000886	537	8	541	14	552	16.7	97
mr17b12	AM2-8	0.08750	0.00060	0.71730	0.00861	0.059430	0.001022	541	7	549	13	582	20.0	93
mr17e05	AM2-37	0.08850	0.00059	0.70560	0.00804	0.057830	0.000746	547	7	542	12	522	13.5	105
mr17f10	AM2-54	0.08880	0.00045	0.73510	0.00654	0.060010	0.000588	549	6	560	10	604	11.8	91
mr17e10	AM2-42	0.08910	0.00048	0.73970	0.00814	0.060190	0.000620	550	6	562	12	610	12.6	90
mr17b11	AM2-7	0.08920	0.00043	0.72480	0.00623	0.058890	0.000536	551	5	553	10	562	10.2	98
mr17e06	AM2-38	0.09020	0.00048	0.74290	0.01047	0.059700	0.000907	557	6	564	16	592	18.0	94
mr17b07	AM2-3	0.09060	0.00053	0.74050	0.00622	0.059260	0.000486	559	6	563	9	576	9.4	97
mr17b14	AM2-10	0.09130	0.00061	0.75780	0.00849	0.060210	0.000668	563	8	573	13	610	13.5	92
mr17e12	AM2-44	0.09120	0.00067	0.74980	0.01635	0.059620	0.001175	563	8	568	25	588	23.2	96
mr17d07	AM2-27	0.09160	0.00062	0.74060	0.01163	0.058650	0.001044	565	8	563	18	554	19.7	102
mr17c14	AM2-22	0.09340	0.00062	0.76730	0.00867	0.059580	0.000697	576	8	578	13	588	13.8	98
mr17f08	AM2-52	0.09360	0.00041	0.78410	0.00917	0.060730	0.000783	577	5	588	14	628	16.2	92
mr17b09	AM2-5	0.09430	0.00054	0.77620	0.00768	0.059700	0.000424	581	7	583	12	592	8.4	98
mr17e09	AM2-41	0.09430	0.00055	0.79570	0.00780	0.061160	0.000636	581	7	594	12	644	13.4	90
mr17e08	AM2-40	0.09710	0.00043	0.81630	0.00555	0.060960	0.000421	597	5	606	8	636	8.8	94
mr17f09	AM2-53	0.09700	0.00043	0.80860	0.00809	0.060430	0.000586	597	5	602	12	618	12.0	97
mr17b13	AM2-9	0.10040	0.00056	0.83580	0.01078	0.060390	0.000791	617	7	617	16	616	16.1	100

mr17d14	AM2-34	0.10200	0.00042	0.88220	0.00618	0.062710	0.000357	626	5	642	9	698	8.0	90
mr17f12	AM2-56	0.10210	0.00065	0.86760	0.01085	0.061590	0.000856	627	8	634	16	658	18.3	95
mr17b16	AM2-12	0.10350	0.00059	0.88920	0.01263	0.062330	0.000885	635	7	646	18	684	19.4	93
mr17b15	AM2-11	0.11380	0.00077	0.97380	0.01032	0.062060	0.000503	695	9	690	15	676	11.0	103
mr17e15	AM2-47	0.15070	0.00062	1.50140	0.00976	0.072230	0.000527	905	7	931	12	992	14.5	91
mr17e11	AM2-43	0.15630	0.00075	1.54170	0.01310	0.071500	0.000579	936	9	947	16	970	15.7	96
mr17c06	AM2-14	0.16720	0.00090	1.67390	0.01557	0.072580	0.000769	997	11	999	19	1002	21.2	100
mr17f15	AM2-59	0.29290	0.00205	4.58910	0.03855	0.113610	0.000534	1656	23	1747	29	1856	17.4	89
mr17e07	AM2-39	0.29700	0.00196	4.50310	0.04368	0.109930	0.000846	1676	22	1732	34	1798	27.7	93
mr17b05	AM2-1	0.32210	0.00110	5.17950	0.01813	0.116590	0.000326	1800	12	1849	13	1904	10.7	95
mr17b05	AM2-1	0.32210	0.00110	5.17950	0.01813	0.116590	0.000326	1800	12	1849	13	1904	10.7	95
mr17c08	AM2-16	0.33340	0.00110	5.41160	0.01840	0.117710	0.000377	1855	12	1887	13	1920	12.3	97
mr17e13	AM2-45	0.33720	0.00189	5.79330	0.03824	0.124590	0.000436	1873	21	1945	26	2022	14.2	93
mr17f11	AM2-55	0.37090	0.00126	6.83810	0.03214	0.133670	0.000615	2034	14	2091	20	2146	19.7	95
mr17e16	AM2-48	0.37170	0.00253	6.98300	0.04958	0.136210	0.000858	2038	28	2109	30	2178	27.4	94
mr17c12	AM2-20	0.46860	0.00253	11.42780	0.05143	0.176860	0.000513	2477	27	2559	23	2622	15.2	94
mr17c11	AM2-19	0.50520	0.00333	13.67910	0.08891	0.196360	0.001060	2636	35	2728	35	2796	30.2	94



Table 4: LA-ICP-MS detrital zircon data of sample LIZ 1, n = 54/60, concordant in the range of 85-115%, a sandstone from the matrix of the Meneage Formation, Gramscatho Group, age of sedimentation is Devonian, Cornwall, Great Britain (sample location: c. 1.3 km north of Porthallow, co-ordinates: 50°04'40" N, 5°04'37" W).

spot	grain	206/238	err	207/235	err	207/206	err	Age206/238	2 $\sigma$	Age207/235	2 $\sigma$	Age207/206	2 $\sigma$	conc/%
mr29g11	LIZ1 43	0.08	0.0018	0.6141	0.027512	0.05567	0.002138	496	22	486	44	438	34	113
mr29g09	LIZ1 41	0.0833	0.001208	0.667	0.019343	0.05805	0.002078	516	15	519	30	530	38	97
mr29f11	LIZ1 31	0.0837	0.000795	0.6625	0.01537	0.05737	0.001279	518	10	516	24	504	22	103
mr29g07	LIZ1 39	0.0837	0.000988	0.6912	0.01493	0.05986	0.00167	518	12	534	23	598	33	87
mr29f12	LIZ1 32	0.085	0.000918	0.6769	0.011575	0.05777	0.001369	526	11	525	18	520	25	101
mr30a14	LIZ1 60	0.0856	0.00083	0.6888	0.009988	0.05835	0.000776	529	10	532	15	542	14	98
mr29d14	LIZ1 10	0.08600	0.0006	0.6843	0.00876	0.05773	0.00088	532	8	529	14	518	16	103
mr29e14	LIZ1 22	0.08600	0.0010	0.6811	0.01430	0.05739	0.00141	532	12	527	22	506	25	105
mr29f06	LIZ1 26	0.0871	0.001028	0.6982	0.018083	0.05811	0.00129	538	13	538	28	532	24	101
mr30a16	LIZ1 62	0.0876	0.000517	0.7156	0.006655	0.05923	0.000432	541	6	548	10	574	8	94
mr29d05	LIZ1 01	0.08770	0.0012	0.7148	0.01930	0.05911	0.00186	542	15	548	30	570	36	95
mr29e10	LIZ1 18	0.08780	0.0006	0.6988	0.01412	0.05773	0.00137	542	7	538	22	518	25	105
mr29e13	LIZ1 21	0.08860	0.0006	0.7240	0.01600	0.05924	0.00134	547	7	553	24	574	26	95
mr29d15	LIZ1 11	0.08900	0.0007	0.7245	0.01101	0.05905	0.00089	549	9	553	17	568	17	97
mr29f10	LIZ1 30	0.0893	0.000688	0.7234	0.010128	0.05875	0.000852	551	8	553	15	556	16	99
mr29g08	LIZ1 40	0.0896	0.000995	0.7048	0.014166	0.05704	0.001112	553	12	542	22	492	19	112
mr29e09	LIZ1 17	0.09010	0.0012	0.7059	0.01574	0.05682	0.00144	556	15	542	24	484	25	115
mr30a05	LIZ1 51	0.0902	0.00074	0.7283	0.012308	0.05857	0.001066	556	9	556	19	550	20	101
mr29e15	LIZ1 23	0.09110	0.0008	0.7341	0.01175	0.05840	0.00095	562	10	559	18	544	18	103
mr29f08	LIZ1 28	0.0922	0.001097	0.7407	0.016814	0.05822	0.001572	569	14	563	26	538	29	106
mr29f07	LIZ1 27	0.0929	0.001338	0.7641	0.018262	0.05966	0.001617	573	17	576	28	590	32	97
mr29g16	LIZ1 48	0.0939	0.001249	0.7939	0.01818	0.06133	0.001257	578	15	593	27	650	27	89
mr29h05	LIZ1 49	0.095	0.001349	0.7777	0.023331	0.05935	0.001608	585	17	584	35	580	31	101
mr30a08	LIZ1 54	0.0969	0.00064	0.8308	0.013791	0.06216	0.001044	596	8	614	20	678	23	88

mr30a09	LIZ1 55	0.097	0.000766	0.8156	0.012805	0.06095	0.000768	597	9	606	19	636	16	94
mr30a11	LIZ1 57	0.0995	0.000935	0.8305	0.009385	0.06052	0.000684	612	12	614	14	622	14	98
mr29e16	LIZ1 24	0.10230	0.0011	0.8550	0.02377	0.06061	0.00176	628	14	627	35	624	36	101
mr29e17	LIZ1 25	1.10230	1.0011	1.8550	1.02377	1.06061	1.00176	629	15	628	36	625	37	102
mr30a10	LIZ1 56	0.1138	0.000728	1.0052	0.00975	0.06406	0.000724	695	9	706	14	742	17	94
mr29e05	LIZ1 13	0.11630	0.0015	1.0551	0.02944	0.06579	0.00220	709	18	731	41	798	53	89
mr29g05	LIZ1 37	0.1728	0.001158	1.7577	0.016347	0.07375	0.00062	1028	14	1030	19	1034	17	99
mr29d08	LIZ1 04	0.24850	0.0019	3.1318	0.03602	0.09137	0.00124	1431	21	1441	33	1454	40	98
mr29f15	LIZ1 35	0.2867	0.002322	4.0855	0.052294	0.10332	0.001467	1625	26	1651	42	1684	48	96
mr29g10	LIZ1 42	0.306	0.002815	4.9147	0.065857	0.11646	0.001607	1721	32	1805	48	1902	52	90
mr29d09	LIZ1 05	0.30900	0.0036	4.7309	0.06434	0.11102	0.00167	1736	40	1773	48	1816	54	96
mr29f09	LIZ1 29	0.3138	0.002071	5.2531	0.091404	0.1214	0.002319	1759	23	1861	65	1976	75	89
mr29e08	LIZ1 16	0.34270	0.0026	5.9168	0.05917	0.12518	0.00101	1900	29	1964	39	2030	33	94
mr29e06	LIZ1 14	0.34330	0.0043	5.9428	0.05467	0.12552	0.00113	1903	48	1968	36	2036	37	93
mr29d10	LIZ1 06	0.34880	0.0020	6.0279	0.04280	0.12530	0.00070	1929	22	1980	28	2032	23	95
mr30a15	LIZ1 61	0.3518	0.003764	6.3153	0.069468	0.13018	0.000794	1943	42	2021	44	2100	26	93
mr29f14	LIZ1 34	0.3533	0.002473	6.0581	0.061793	0.12432	0.000982	1950	27	1984	40	2018	32	97
mr29d12	LIZ1 08	0.35410	0.0019	5.9738	0.02330	0.12233	0.00045	1954	21	1972	15	1990	15	98
mr29e07	LIZ1 15	0.35580	0.0025	6.0685	0.04794	0.12367	0.00088	1962	27	1986	31	2008	29	98
mr29g13	LIZ1 45	0.3579	0.002219	6.3404	0.05643	0.12845	0.001066	1972	24	2024	36	2076	34	95
mr29d13	LIZ1 09	0.35880	0.0025	6.0575	0.05997	0.12243	0.00132	1976	28	1984	39	1992	43	99
mr29g12	LIZ1 44	0.3596	0.002805	6.401	0.06593	0.12907	0.001394	1980	31	2032	42	2084	45	95
mr30a12	LIZ1 58	0.3656	0.005374	6.5054	0.088473	0.12901	0.000864	2009	59	2047	56	2084	28	96
mr29d11	LIZ1 07	0.37670	0.0016	6.7777	0.04406	0.13047	0.00091	2061	17	2083	27	2104	29	98
mr29f16	LIZ1 36	0.3862	0.003399	7.1264	0.065563	0.13379	0.001191	2105	37	2127	39	2148	38	98
mr29d16	LIZ1 12	0.39280	0.0028	7.1248	0.06341	0.13152	0.00112	2136	30	2127	38	2118	36	101
mr29g15	LIZ1 47	0.4415	0.004636	10.3124	0.117561	0.16937	0.001728	2357	49	2463	56	2550	52	92
mr30a13	LIZ1 59	0.4729	0.00558	11.6886	0.149614	0.17922	0.000914	2496	59	2580	66	2644	27	94

mr29d06	LIZ1 02	0.49230	0.0022	12.0694	0.07121	0.17777	0.00114	2581	23	2610	31	2632	34	98
mr29h06	LIZ1 50	0.4952	0.003764	12.1739	0.080348	0.17827	0.000874	2593	39	2618	35	2636	26	98



Table 5: LA-ICP-MS detrital zircon data for sample LIZ 3,  $n = 50/60$ , concordant in the range of 85-115%, a Lower Ordovician quartzite block in the Meneage Formation, Gramscatho group, age of sedimentation is Devonian, Cornwall, Great Britain (sample location c. 1.3 km north of Porthallow, co-ordinates: 50°04'41" N, 5°04'40" W).

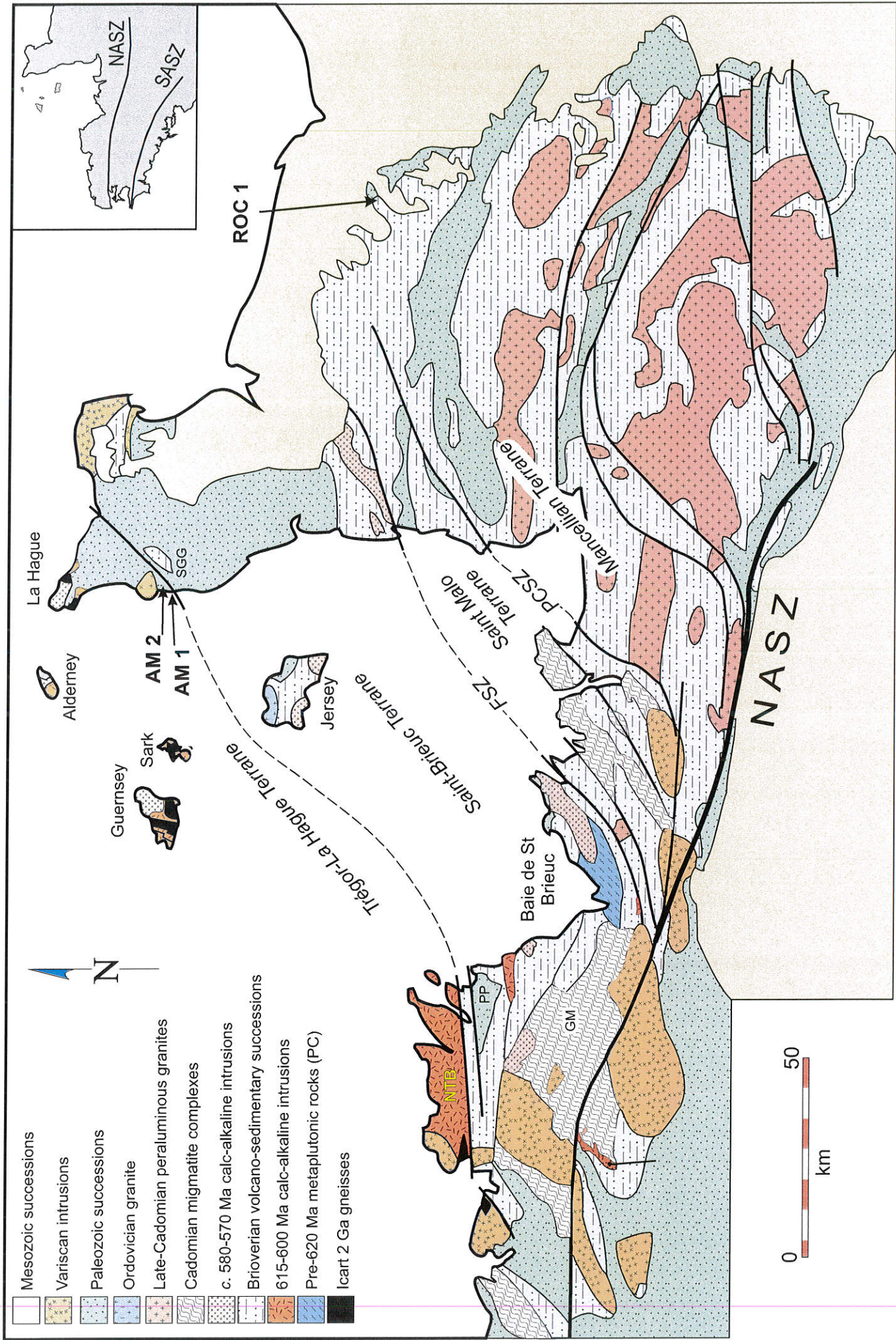
spot	grain	206/238	err	207/235	err	207/206	err	Age206/238	2 $\sigma$	Age207/235	2 $\sigma$	Age207/206	2 $\sigma$	conc%
mr30f10	LIZ3 54	0.08590	0.00040	0.71400	0.00743	0.06029	0.00065	531	5	547	11	614	13	86
mr30f08	LIZ3 52	0.08820	0.00052	0.72960	0.00635	0.05996	0.00050	545	6	556	10	602	10	91
mr30f13	LIZ3 57	0.08830	0.00126	0.73510	0.01779	0.06036	0.00171	545	16	560	27	616	35	88
mr30e16	LIZ3 48	0.08830	0.00097	0.70520	0.01446	0.05788	0.00100	546	12	542	22	524	18	104
mr30c11	LIZ3 19	0.08870	0.00084	0.72840	0.01042	0.05955	0.00082	548	10	556	16	586	16	94
mr30f11	LIZ3 55	0.08870	0.00073	0.71990	0.01476	0.05882	0.00126	548	9	551	23	560	24	98
mr30e05	LIZ3 37	0.08960	0.00037	0.73040	0.00993	0.05912	0.00073	553	5	557	15	570	14	97
mr30e09	LIZ3 41	0.09130	0.00075	0.72060	0.00894	0.05725	0.00071	563	9	551	14	500	12	113
mr30f09	LIZ3 53	0.09200	0.00069	0.75780	0.00599	0.05972	0.00053	567	9	573	9	592	11	96
mr30b10	LIZ3 06	0.09220	0.00065	0.74940	0.00794	0.05892	0.00071	569	8	568	12	564	14	101
mr30b12	LIZ3 08	0.09280	0.00049	0.78390	0.01121	0.06123	0.00097	572	6	588	17	646	20	89
mr30f12	LIZ3 56	0.09340	0.00056	0.79770	0.01125	0.06192	0.00104	576	7	596	17	670	23	86
mr30d08	LIZ3 28	0.09360	0.00122	0.77050	0.01264	0.05968	0.00113	577	15	580	19	592	22	97
mr30d11	LIZ3 31	0.09590	0.00074	0.78980	0.00940	0.05971	0.00077	590	9	591	14	592	15	100
mr30b14	LIZ3 10	0.09630	0.00079	0.77500	0.00922	0.05834	0.00075	593	10	583	14	542	14	109
mr30c12	LIZ3 20	0.09660	0.00046	0.81670	0.00604	0.06131	0.00045	594	6	606	9	650	10	91
mr30c05	LIZ3 13	0.09680	0.00103	0.81010	0.01118	0.06069	0.00098	596	13	602	17	628	20	95
mr30c10	LIZ3 18	0.09710	0.00123	0.83480	0.01052	0.06235	0.00054	597	15	616	16	684	12	87
mr30f06	LIZ3 50	0.09700	0.00085	0.80660	0.00807	0.06027	0.00080	597	11	601	12	612	16	98
mr30e11	LIZ3 43	0.09720	0.00068	0.81540	0.01402	0.06083	0.00086	598	8	605	21	632	18	95
mr30b09	LIZ3 05	0.09750	0.00098	0.81420	0.00814	0.06053	0.00045	600	12	605	12	622	9	96
mr30f15	LIZ3 59	0.09790	0.00083	0.82570	0.01148	0.06116	0.00077	602	10	611	17	644	16	93
mr30b13	LIZ3 09	0.09830	0.00065	0.81790	0.01325	0.06035	0.00101	604	8	607	20	616	21	98



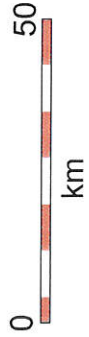
mr30e15	LIZ3 47	0.09870	0.00083	0.83280	0.00974	0.06120	0.00085	607	10	615	14	646	18	94
mr30e12	LIZ3 44	0.09900	0.00130	0.83710	0.02202	0.06134	0.00202	608	16	618	33	650	43	94
mr30c07	LIZ3 15	0.09910	0.00095	0.82400	0.00923	0.06030	0.00056	609	12	610	14	614	11	99
mr30c08	LIZ3 16	0.09920	0.00117	0.81500	0.01190	0.05956	0.00075	610	14	605	18	586	15	104
mr30d14	LIZ3 34	0.09960	0.00110	0.80720	0.01203	0.05874	0.00089	612	13	601	18	556	17	110
mr30f05	LIZ3 49	0.10000	0.00160	0.83160	0.01547	0.06028	0.00128	615	20	615	23	612	26	100
mr30b11	LIZ3 07	0.10030	0.00055	0.85190	0.00912	0.06159	0.00070	616	7	626	13	658	15	94
mr30e13	LIZ3 45	0.10040	0.00069	0.82380	0.00865	0.05948	0.00049	617	9	610	13	584	10	106
mr30c14	LIZ3 22	0.10050	0.00045	0.85430	0.00991	0.06161	0.00076	618	6	627	15	660	16	94
mr30d06	LIZ3 26	0.10220	0.00069	0.85170	0.01243	0.06044	0.00080	627	9	626	18	618	16	101
mr30d10	LIZ3 30	0.10280	0.00081	0.85560	0.00992	0.06038	0.00073	631	10	628	15	616	15	102
mr30e06	LIZ3 38	0.10300	0.00090	0.86520	0.01324	0.06091	0.00088	632	11	633	19	634	18	100
mr30e14	LIZ3 46	0.10320	0.00080	0.83960	0.01259	0.05898	0.00084	633	10	619	19	566	16	112
mr30d16	LIZ3 36	0.10550	0.00111	0.88190	0.01429	0.06063	0.00061	646	14	642	21	626	13	103
mr30b08	LIZ3 04	0.23070	0.00134	3.03080	0.01970	0.09527	0.00048	1338	16	1415	18	1532	15	87
mr30e10	LIZ3 42	0.25900	0.00137	3.36180	0.01883	0.09411	0.00062	1485	16	1496	17	1510	20	98
mr30f07	LIZ3 51	0.28960	0.00252	4.25610	0.06469	0.10658	0.00175	1639	29	1685	51	1740	57	94
mr30d09	LIZ3 29	0.31670	0.00200	4.76850	0.03719	0.10919	0.00083	1773	22	1779	28	1786	27	99
mr30d15	LIZ3 35	0.33840	0.00220	5.57540	0.04962	0.111947	0.00084	1879	24	1912	34	1948	27	96
mr30e07	LIZ3 39	0.34860	0.00108	6.02620	0.02410	0.12535	0.00043	1928	12	1980	16	2032	14	95
mr30c09	LIZ3 17	0.35990	0.00281	6.36850	0.05732	0.12832	0.00053	1982	31	2028	37	2074	17	96
mr30b07	LIZ3 03	0.36980	0.00203	6.69010	0.03479	0.13118	0.00072	2028	22	2071	22	2112	23	96
mr30d05	LIZ3 25	0.37190	0.00271	6.71230	0.03759	0.13088	0.00052	2038	30	2074	23	2108	17	97
mr30d13	LIZ3 33	0.37740	0.00226	7.20060	0.06913	0.13836	0.00116	2064	25	2137	41	2206	37	94
mr30f16	LIZ3 60	0.41140	0.00288	8.55520	0.13175	0.15080	0.00256	2221	31	2292	71	2354	80	94
mr30b05	LIZ3 01	0.43290	0.00212	9.62040	0.07504	0.16114	0.00151	2319	23	2399	37	2466	46	94
mr30c15	LIZ3 23	0.50630	0.00238	13.59410	0.06117	0.19471	0.00051	2641	25	2722	24	2782	14	95







- Mesozoic successions
- Variscan intrusions
- Paleozoic successions
- Ordovician granite
- Late-Cadomian peraluminous granites
- Cadomian migmatite complexes
- c. 580-570 Ma calc-alkaline intrusions
- Brioverian volcano-sedimentary successions
- 615-600 Ma calc-alkaline intrusions
- Pre-620 Ma metaplutonic rocks (PC)
- Icart 2 Ga gneisses



La Hague

Alderney

Guernsey

Sark

AM 2

AM 1

SGG

ROC 1

Jersey

Tregor-La Hague Terrane

Saint-Malo Terrane

Baie de St Brieuc

Marcellian Terrane

NASZ

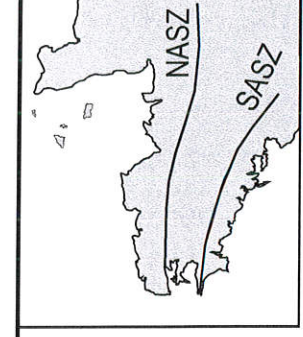
GM

PP

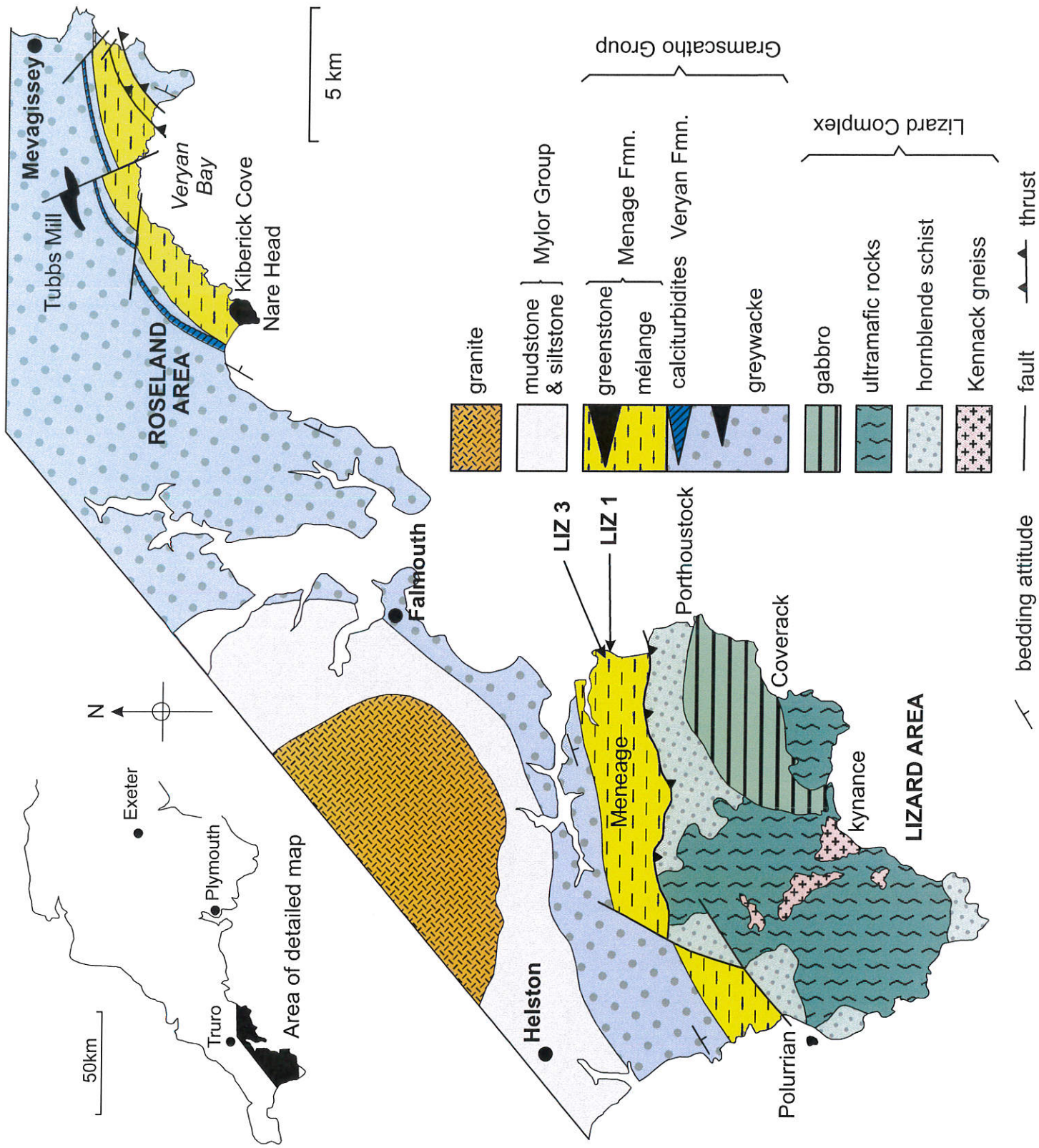
PCSZ

FSZ

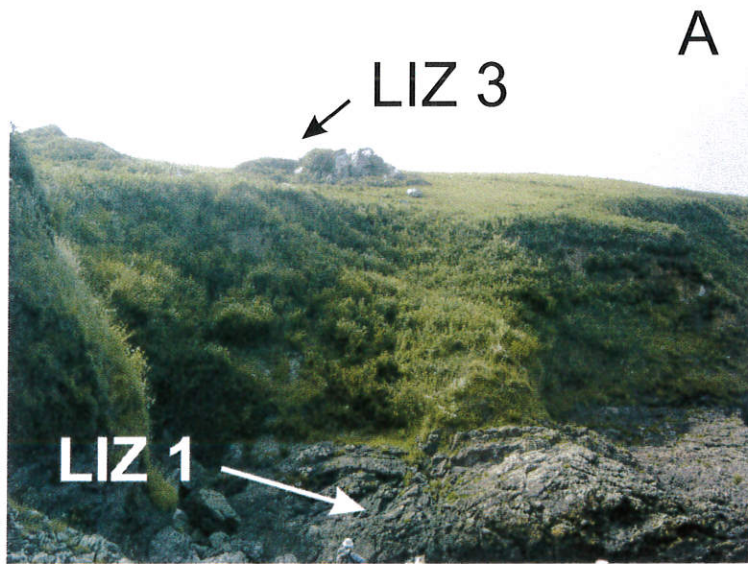
NTB







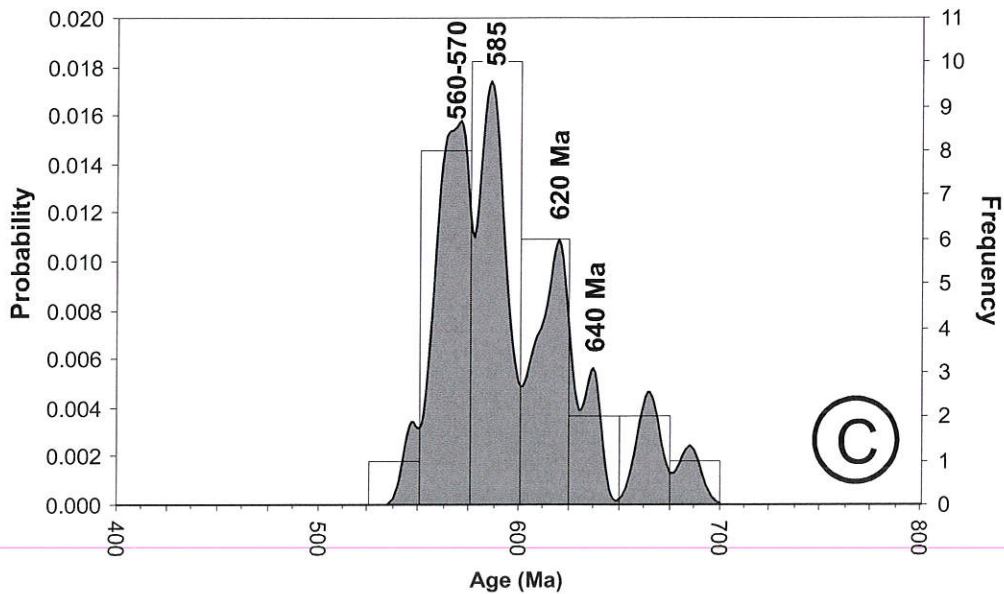
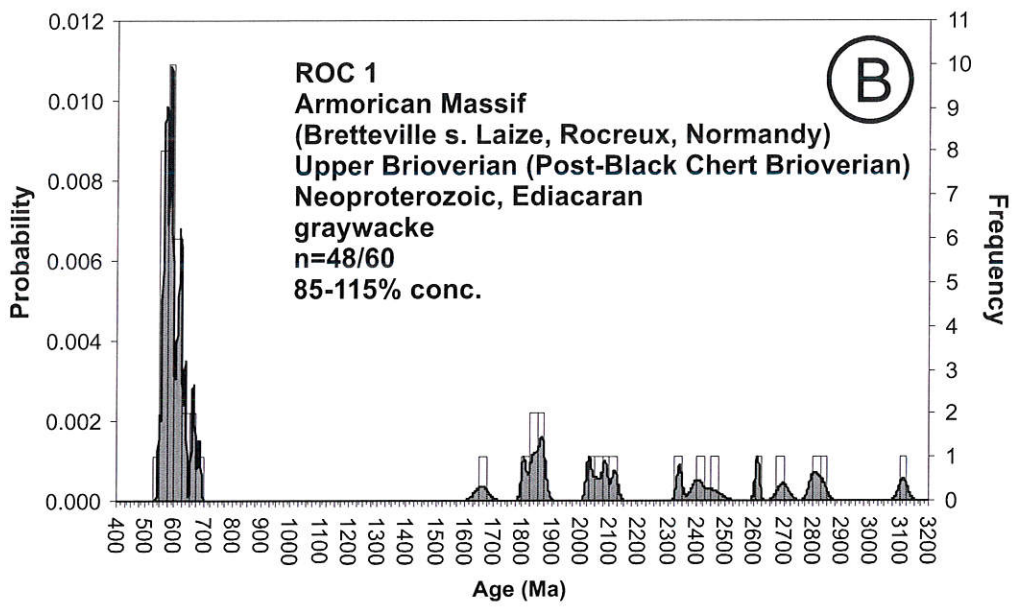
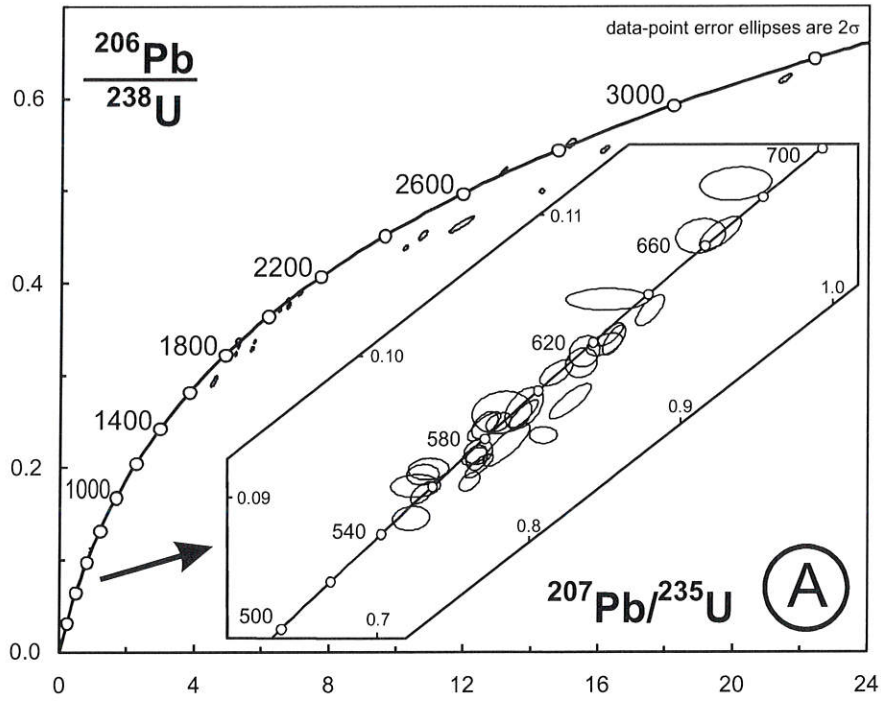


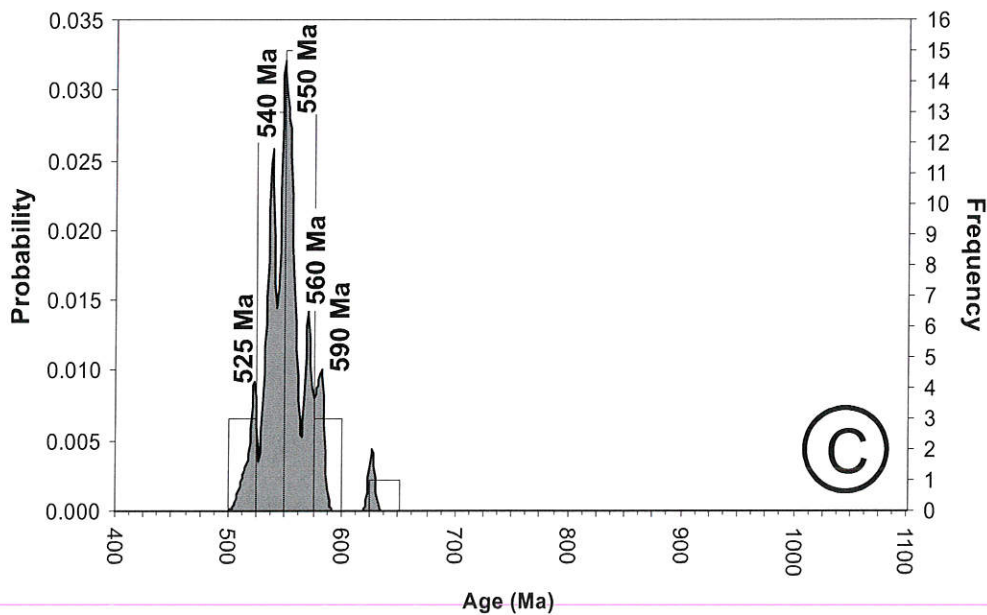
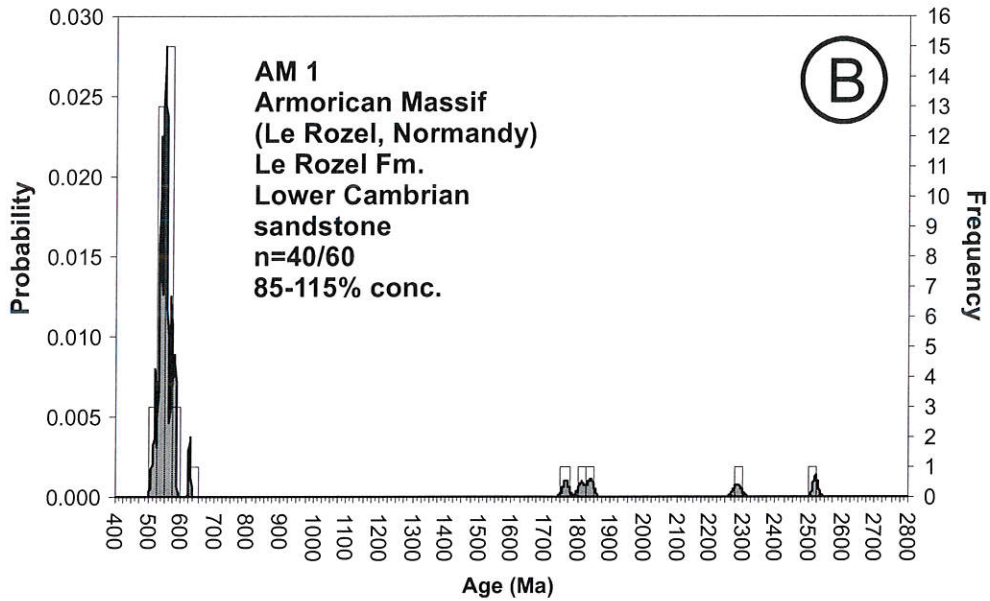
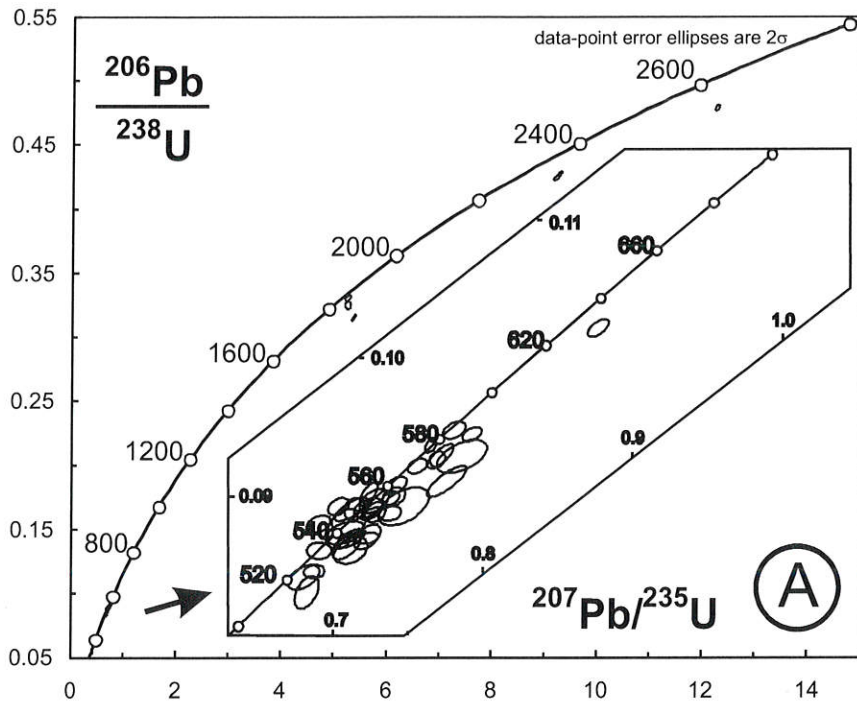


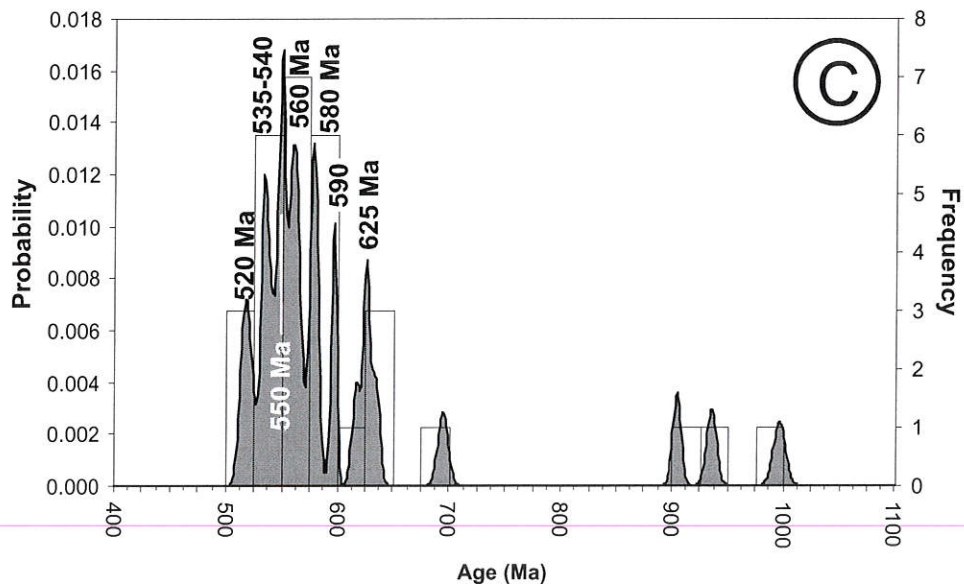
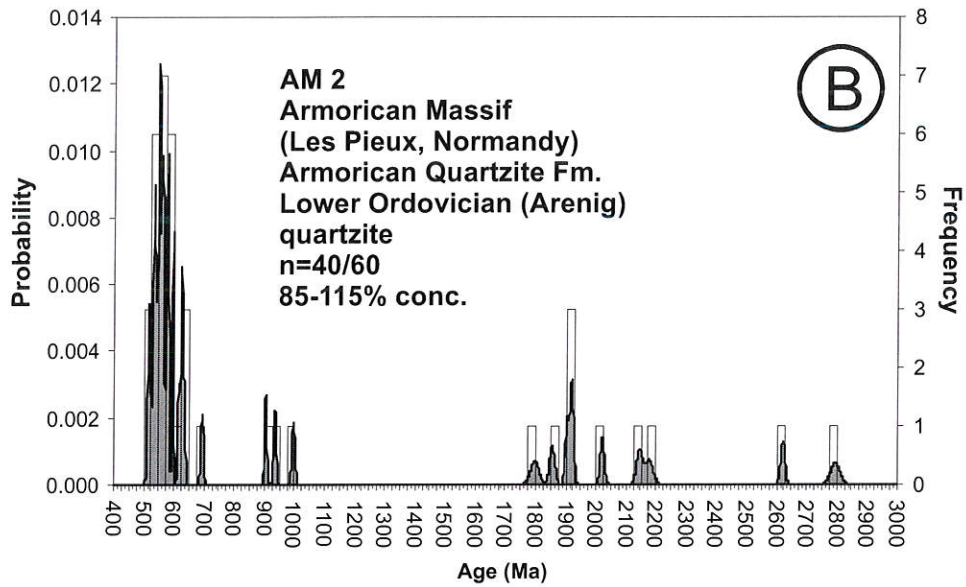
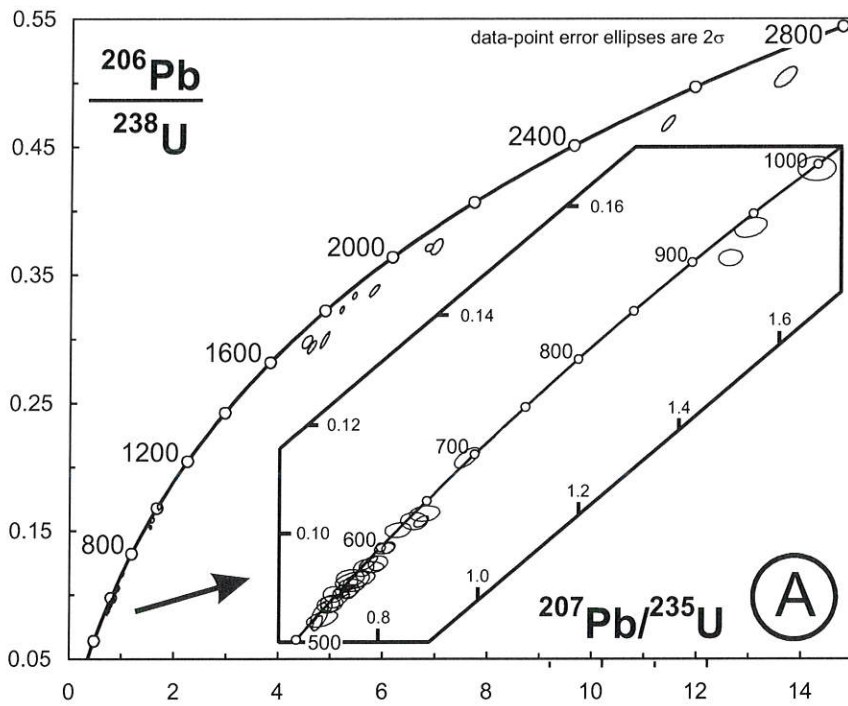




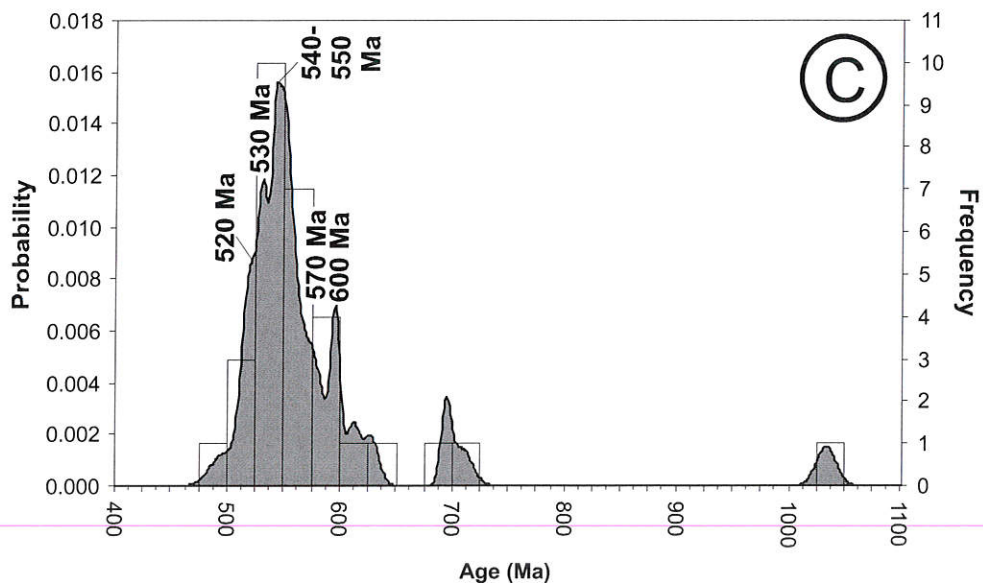
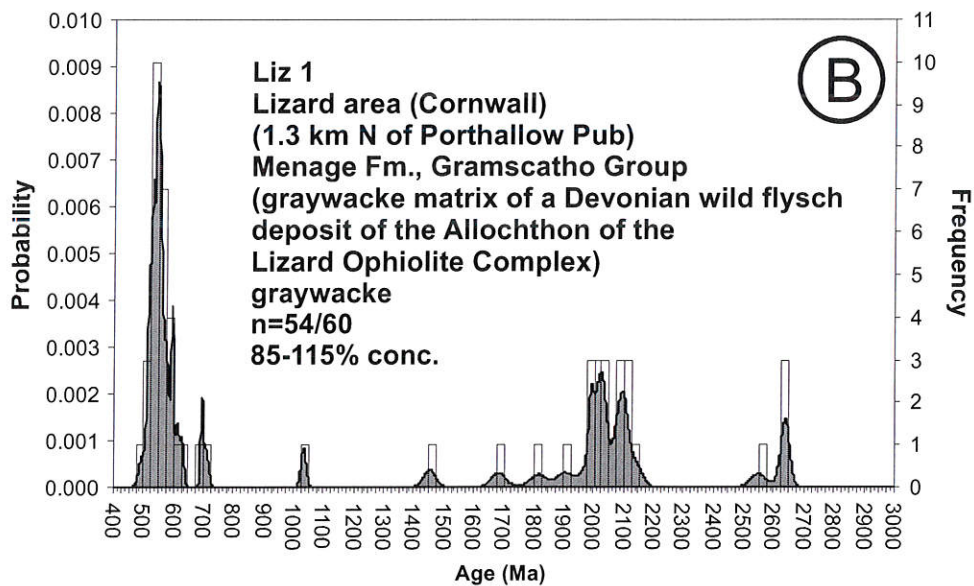
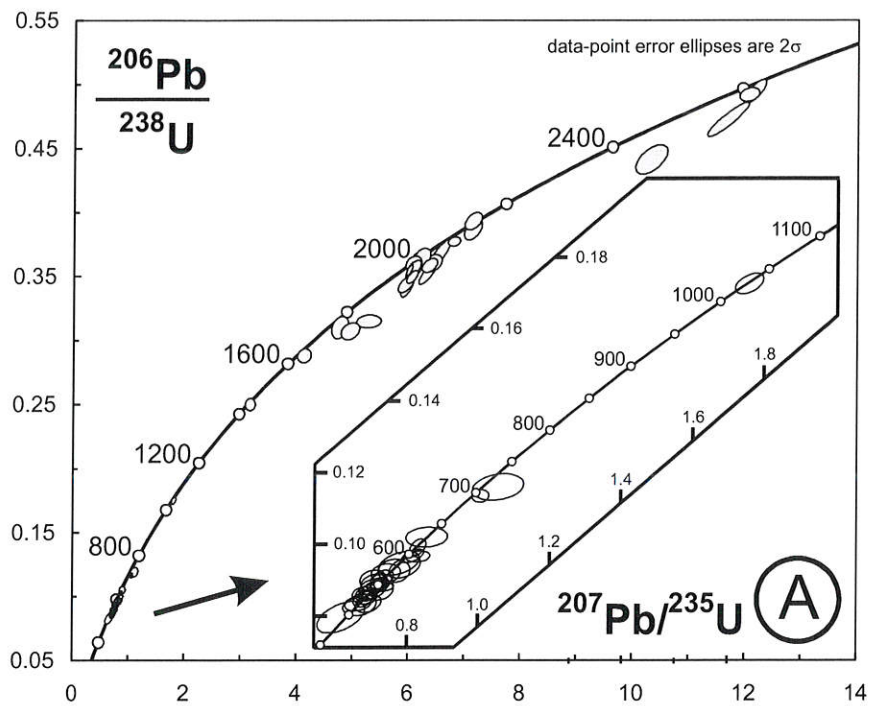


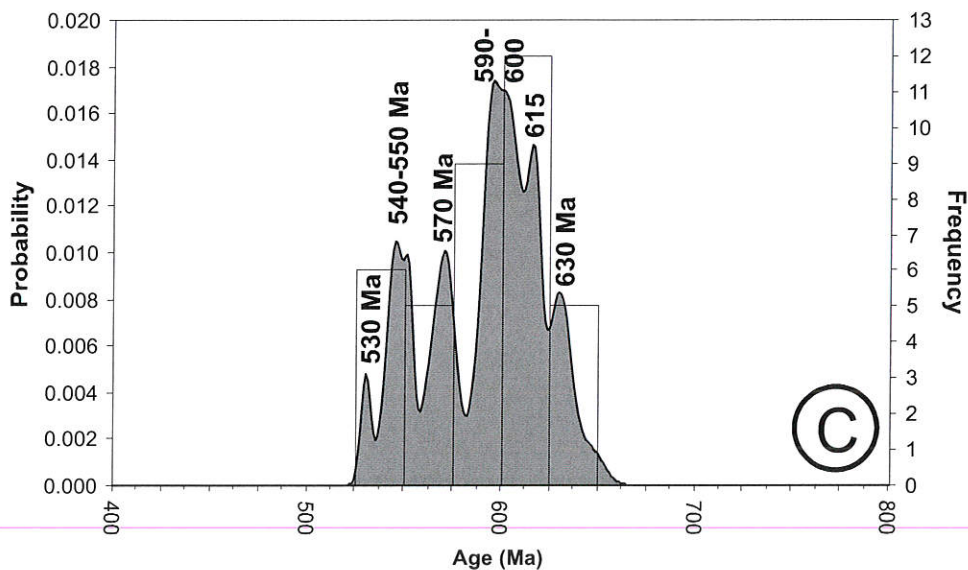
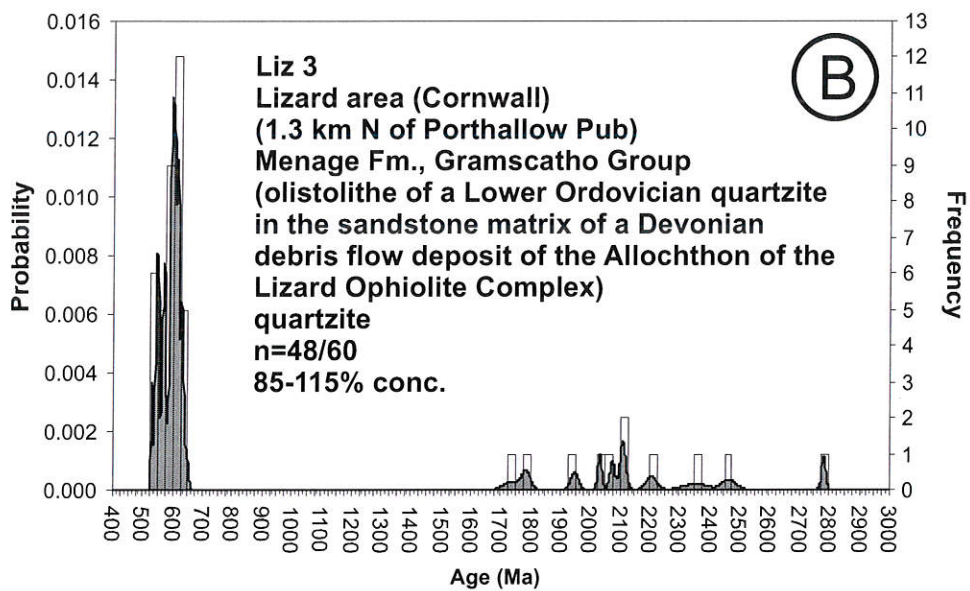
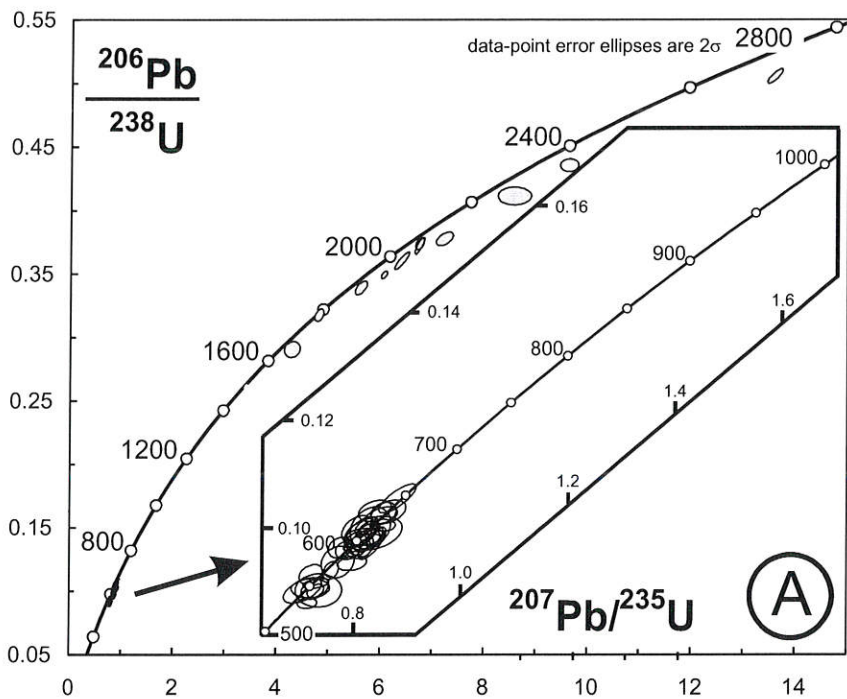




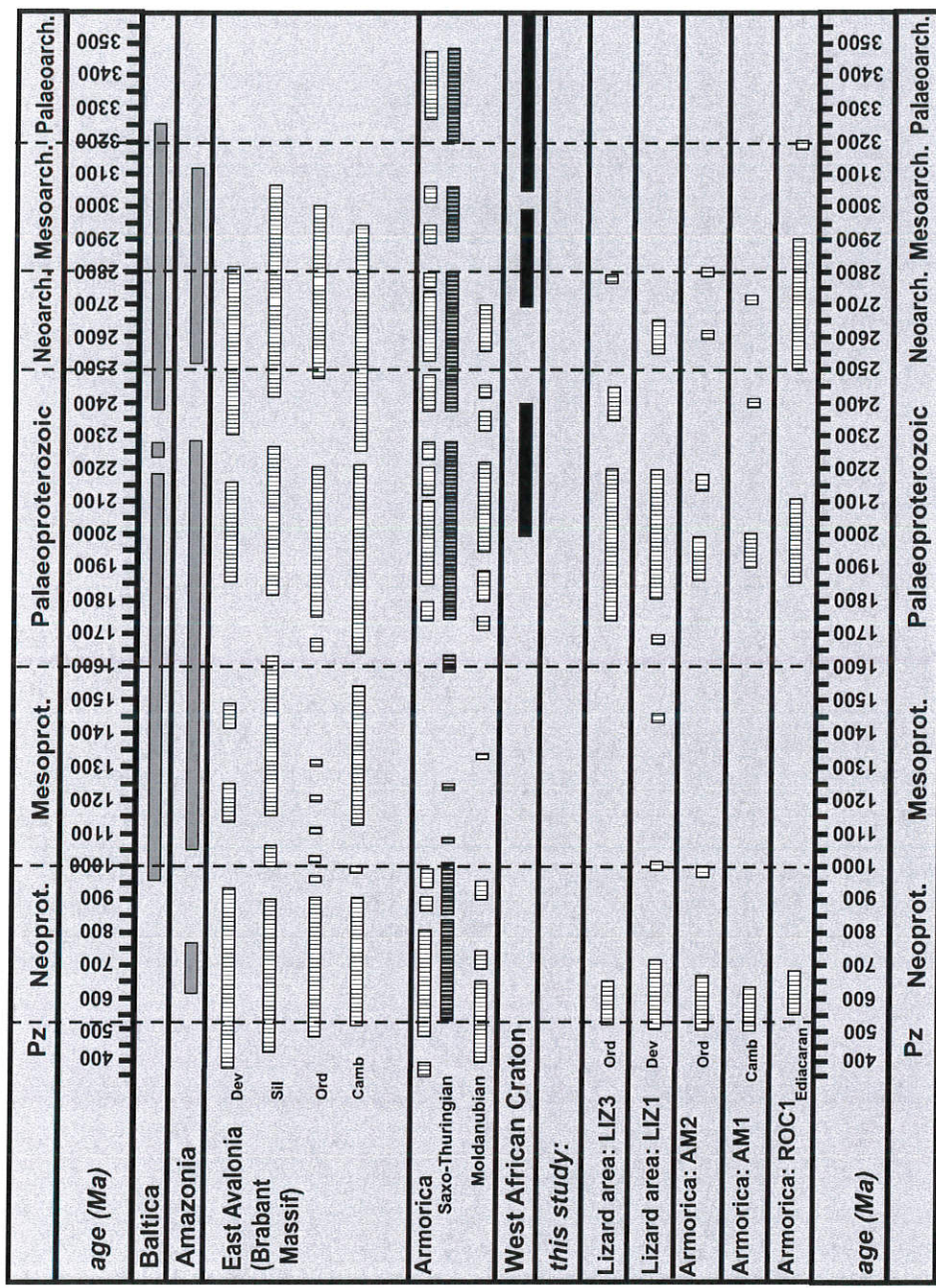












Dev - Devonian  
 Sil - Silurian  
 Ord - Ordovician  
 Cam - Cambrian  
 Pz - Palaeozoic



NNW

SSE

